Detoxification gene families in Phylloxera: Endogenous functions and roles in response to the environment

Thomas Chertemps, Gaëlle Le Goff, Martine Maïbèche, Frédérique Hilliou

Version of Record: https://www.sciencedirect.com/science/article/pii/S1744117X21000794
Manuscript_689c20f4c0e2170088c0c028ad936c02

Running Title: Detoxification gene families in Phylloxera

Option long

Detoxification gene families in Phylloxera: endogenous functions and roles in response to the environment

Authors

Thomas Chertemps[1*], Gaëlle Le Goff[2*], Martine Maïbèche[1*] and Frédérique Hilliou[2]**

1: Sorbonne Université, UPEC, Université Paris 7, INRAE, CNRS, IRD, Institute of Ecology and Environmental Sciences, Paris, France.

2: Université Côte d'Azur, INRAE, CNRS, ISA, 400 Route des Chappes, 06903, Sophia Antipolis, France.

*: these authors equally contribute

**: corresponding author, Frederique.hilliou@inrae.fr

Abstract

Phylloxera, *Daktulosphaira vitifoliae*, is an agronomic pest that feeds monophagously on grapevine, *Vitis* spp. host plants. Phylloxera manipulates primary and secondary plant metabolism to establish either leaf or root galls. We manually annotated 198 detoxification genes potentially involved in plant host manipulation, including cytochrome P450 (66 CYPs), carboxylesterase (20 CCEs), glutathione-S-transferase (10 GSTs), uridine diphosphate-glycosyltransferase (35 UGTs) and ABC transporter (67 ABCs) families. Transcriptomic expression patterns of these detoxification genes were analyzed for root and leaf galls. In addition to these transcriptomic analyses, we reanalyzed recent data from L1 and L2-3 stages feeding on tolerant and resistant rootstock. Data from two agricultural pest aphids, the generalist *Myzus persicae* and the Fabaceae specialist *Acyrthosiphon pisum,* and from the true bug vector of Chagas disease, *Rhodnius prolixus,* were used to perform phylogenetic analyses for each detoxification gene family. We found expansions of several gene sub-families in the genome of *D. vitifoliae.* Phylogenetically close genes were found to be organized in clusters in the same genomic position and orientation suggesting recent successive duplications. These results highlight the roles of the phylloxera detoxification gene repertoire in insect physiology and in adaptation to plant secondary metabolites, and provide gene candidates for further functional analyses.

Keywords: adaptation, detoxification, *Daktulosphaira vitifoliae*, insect hormones, omics

Introduction

Daktulosphaira vitifoliae is better known as phylloxera, the pest responsible for the massive European vineyard destruction in the XIXth century. *D. vitifoliae* is a piercing-sucking monophagous hemipteran. Phylloxera feeds on *Vitis* spp. host plants, forms galls and highjacks plant resources for its own benefit (Forneck et al., 2001, Kellow et al., 2004, Nabity et al., 2013). The polyphenic phylloxera life cycle has several generations per year and different insect forms feed on leaves (gallicole, GA) and roots (radicicole, RA; Figure 1) (Powell et al., 2013).

In plants, primary metabolism responds to phylloxera attack with enhanced levels of free amino acids, particularly glutamine (Kellow et al., 2004). Phylloxera infests grapevine hosts by inhibiting water- and mineral-uptake, modifying sink-source translocation, altering secondary metabolism and manipulating root growth (Eitle et al., 2017). While phylloxera resistance to pesticides is rarely reported, several studies have demonstrated phylloxera interactions and/or manipulations of plant secondary metabolites (Du et al., 2009, Eitle et al., 2017, Kellow et al., 2004, Nabity et al., 2013, Powell et al., 2013). Insect adaptation to plants they fed on partly relies on detoxification genes (Dermauw et al., 2018). Detoxification gene products are targets for xenobiotics which include plant secondary products and chemical compounds such as pesticides. Two naturally occurring phenolic compounds in grapevine, chlorogenic acid and quercetin, stimulate gall formation, whereas caffeic acid, quinic acid and glycosylated quercetin appear to inhibit gall formation in resistant hybrids (Denisova, 1965, Powell et al., 2013). Data suggest that phylloxera might also manipulate plant hormones since an auxin is found in phylloxera saliva (Schaller, 1963) and levels of other hormones (abscisic acid, zeatin, gibberellic acid, cytokinins, kinetin) are induced during gall formation in leaf and root galls. The GA and RA forms of phylloxera specifically manipulate plant organ physiology but little is known about insect physiological changes during this plant-insect interaction.

GA and RA forms have specific patterns of host plant manipulation. After root attack, levels of terpenoid pathway compounds increased (Lawo et al., 2011), possibly due to up-regulation of mevalonate and/or alternative isopentenyl pyrophosphate pathways (IPP). Plant secondary metabolite profiles differ between young nodosities and mature nodosities during phylloxera root infection. Beta-caryophyllene is only found in mature nodosities and is induced in response to root attack where it attracts natural plant enemies (Rasmann et al., 2005). Phenylpropanoid pathway compounds l are elevated in mature compared to young nodosities (Loughrin et al., 1997). The lipoxygenase pathway is also induced following phylloxera attack and high levels of linoleic acid were measured in resistant grapevine (Du et al., 2009, Tucker et al., 2007). As a consequence, volatiles derived fromthe mevalonate and IPP pathways and the compounds from phenylpropanoid pathway (phenolics, flavonoids and stilbenes) are also up-regulated in roots of grapevines infected by the radicicole form (Du et al., 2009, Lawo et al., 2011). Flavonol compounds, such as rutin and quercetin glycoside, were up-regulated in leaf tissue after root attack (Benheim et al., 2011), together with a reduction in chlorophyll content and an increase in xanthophyll protective pigments and other carotenoids (Düring, 1999).

Phylloxera leaf galls predominantly occur on non-economically important American *Vitis* hosts, and in southern Europe, leaf galling is more common than root-galling (Powell et al 2013). Leaf galling on *V. vinifera* is associated with enhanced auxin levels such as indole acetic acid (Powell et al., 2013). Transcriptomic analyses of GA and RA are helping us understand phylloxera adaptation to its *Vitis* hosts, and a recent study of phylloxera leaf gall development suggested that phylloxera is redirecting leaf development to carpel formation (Schultz et al., 2019). GA forms suppressed accumulation of gibberellins, auxins and jasmonate in early stages of plant gall development, and abscisic acid was barely detectable in plant galls (Body et al., 2019). Cytokinins play a central role in the initiation of plant galls, but at the early stage of plant gall development, the plant pathway is not activated implying that phylloxera could provide this phytohormone. Phylloxera could manipulate other phytohormones and plant biosynthetic pathways. Here, we quantify detoxification gene expression levels in RA and GA in order to characterize phylloxera responses to *Vitis* species.

Xenobiotic detoxification requires three phases: an initial oxidation-reduction-hydrolysis (mainly cytochrome P450s (CYP) and carboxylesterases (CCE)), followed by enzymatic conjugation (UDP-glycolsyl transferases (UGT) or glutathione S-transferases (GST)) and finally, conjugated-metabolite transport-excretion out of the cells (ABC transporters (ABC)). Many insect CYPs are involved in the metabolism of key endogenous substrates such as steroid hormones and lipids. CYPs are also associated with the metabolism or detoxification of xenobiotics such as plant natural products and pesticides and are key components for the insects' successful adaptation to their host plants (Heidel-Fischer and Vogel, 2015). Carboxylesterase (Pfam PF00135 domain) is a gene family belonging to the α/β hydrolase protein superfamily (Pfam PF00561 domain) (Oakeshott et al., 2005). The CCE family comprises mostly catalytic proteins that hydrolyze a number of carboxylic esters but there are non-catalytic exceptions (Oakeshott et al., 2010, Oakeshott et al., 2005). CCEs are also involved in the modification of insect juvenile hormone, an endogenous sesquiterpene. Glutathione S-transferases (EC 2.5.1.18, GSTs), and the uridine diphosphate-glycosyltransferases (EC 2.4.1.17, UGTs) (Jakoby and Ziegler, 1990) are conjugation enzymes that covalently attach small endogenous hydrophilic molecules to increase compound solubility and facilitate their excretion. GSTs can be divided into several classes based on their cellular localizations (cytosolic or microsomal), substrate specificities and phylogenetic relationships. UGTs catalyze the conjugation of a glycosyl group from a UDP-glycoside to variety of small hydrophobic molecules (lipophilic aglycones), resulting in highly hydrophilic molecules that are subsequently eliminated by excretion pathways or sequestered as non-toxic compounds (Bozzolan et al., 2014). In insects, UGTs are involved in the metabolization of

several allelochemical compounds (Huang et al., 2008), and appear to play a role in insecticide resistance mechanisms (Pedra et al., 2004, Silva et al., 2012, Vontas et al., 2005, Yang et al., 2013). ATP-binding cassette transporters use ATP hydrolysis energy to transport substrates like amino acids, lipids, peptides, sugars and drugs across cell membranes. In insects, they have attracted recent interest due to their involvement in insecticide resistance.

Here, we investigate the potential roles of phylloxera detoxification genes in adaptation to *Vitis* species. Our study is based on the manual annotation of detoxification genes from previously named families using the recently published genome of *D. vitifoliae* (Rispe et al., 2020). Using RNAseq data from GA and RA whole bodies (Rispe et al., 2016), we inferred expression levels associated with the suite of detoxification genes. We also re-analyzed transcriptomic data from L1 and L2-3 phylloxera stages feeding on tolerant and resistant rootstock (Savoi et al., 2020). By combining genomic information, orthology studies, phylogenetic and expression data, we were able to infer potential roles of certain detoxification genes in the response of specialist phylloxera to both its main host, *Vitis vinifera*, and to insect endogenous compounds. We highlight the role of key detoxification gene targets for future functional studies to confirm their involvement phylloxera-grapevine adaptive interactions.

Results-discussion

D. vitifoliae divergence from the piercing-sucking hemipteran pea aphid *Acyrthosiphon pisum* or green peach aphid, *Myzus persicae* occurred about 137 MYA*,* and from the Chagas disease vector *Rhodnius prolixus* at 302 MYA. *A. pisum*, *M. persicae* and *R. prolixus* have sequenced genomes with manually annotated detoxification gene families (Ramsey et al., 2010, Schama et al., 2016) and serve as comparison for our studies. *A. pisum* is a Fabaceae specialist and *M. persicae* is a broad generalist (Blackman and Eastop 2000). *D. vitifoliae* detoxification genes were identified in the recently published genome, manually annotated and compared with family members from these three species. We found 66 CYPs, 20 CCEs, 35 UGTs, 10 GSTs, and 67 ABCs in the *D. vitifoliae* genome (Table 1) (Rispe et al., 2020), and heterogeneity in detoxification gene numbers among the annotated hemipteran genomes. For example, the invasive polyphagous glasshouse white fly, *Trialeurodes vaporariorum* displayed 2.6 times more GSTs and 1.4 less ABCs than phylloxera.

Phase I enzymes: CYP and CCE

CYP

66 CYP sequences were found on 56 scaffolds with 30% of these containing more than one CYP. CYP genes are often clustered in genomes, as a result of gene duplication events (Feyereisen, 2011b). Suppl Table 1 summarizes the scaffold, gene position, orientation, exon number, protein size, clan and the name attributed by David Nelson. Based on their sequence identity, we annotated 7, 20, 33 and 6 members for CYP2, CYP3, CYP4 and mitochondrial clades, respectively. The phylogeny of the 66 DvCYPs, is presented in Figure 2A. Mitochondrial and CYP2 clans are evolutionary conserved in Hemiptera and have roles in insect development , but they are also involved in chemosensory processes (Willingham and Keil, 2004, Feyereisen, 2012). Five CYP2 clade members had a 1:1 ortholog in the *A. pisum* and *M. persicae* genomes. A single copy of CYP307A was found in *D. vitifoliae* and *A. pisum* compare to two copies in *M. persicae*. A single copy of CYP15A was found in *D. vitifoliae* versus three copies for *M. persicae* and *A. pisum* (Mathers et al., 2017). CYP15A catalyzes the epoxidation of methyl farnesoate to juvenile hormone (Helvig et al., 2004) and CYP307A2 is involved in the ecdysone pathway. DvCYP15A1 and DvCYP307A2 are thus most probably involved in

molting, which is consistent with their low expression in phylloxera adult GA and RA forms (Schumann et al., 2018b). Ecdysteroidogenic P450 expression levelscorresponding to*Halloween* genes are summarized in Figure 3. CYP18A1 (ecdysteroid inactivating enzyme) and CYP306A1 , clustered on scaffold52, are highly expressed in the two adult forms. It has been suggested that the CYP306A1 whitefly ortholog might be also involved in adaptation to plant secondary metabolites, like the alkaloid nicotine (Pym et al., 2019). Only one copy of CYP314A1 was found in *D. vitifoliae* whereas three copies were found in *A. pisum* and two in *M. persicae*. The *D. melanogaster* CYP314A1 enzyme catalyzes the hydroxylation of ecdysone to the steroid insect molting hormone 20-hydroxyecdysone (Petryk et al., 2003). DvCYP314A1 is expressed at higher levels in RA than in GA. DvCYP302A1, also involved in 20-hydroxyecdysone biosynthesis, had one ortholog in *M. persicae* while *A. pisum* had two (Ramsey et al., 2010).

D. vitifoliae possessed one copy of CYP303A1, one of the rare 1:1 CYP orthologs in insects. It is essential for adult eclosion a function conserved over 400MY in *D. melanogaster* and *Locusta migratoria* (Wu et al., 2019). Its gene product is involved in the regulation of cuticular hydrocarbon synthesis protecting insects from water loss and insecticide penetration in locust (Wu et al., 2020)... In drosophila, CYP303A1 is essential for wing extension at adult eclosion. We estimated that DvCYP303A1 expression is 7-times higher in RA compared to GA forms (Figure 2B) suggesting a specific role in the root environment. Interestingly, winged-phylloxera forms emerge from radicicole forms.

In insects, CYP3 clade members are involved in xenobiotic metabolism and insecticide resistance. The CYP4 clade is a highly diversified group of enzymes involved in pesticide metabolism, development and chemical communication. Both clades showed more diversity than CYP2 and mitochondrial clades when compared to *M. persicae* and *A. pisum* (Table 1)**.** The *CYP6CZ* family (4 members) showed an expansion compared to *A. pisum* and *M. persicae*, which each contain a single *CYP6CZ*. Two CYP6CZ are clustered on scaffold 184 (Suppl data Figure1) in close proximity with two effectors, which are small secreted proteins potentially essential for interactions between phylloxera and grapevines, five ABC transporters, two genes involved in development and a glutamate receptor. The other two CYP6CZ members are clustered on scaffold 156 (Suppl data Figure 2) withCYP6CZ2 highly expressed in GA forms (Figure 2B, Suppl data Figure 2). CYP6CZ2 is up-regulated in the phylloxera feeding larval stage compared to the probing stage. In contrast, CYP6CZ3 is expressed more highly in the L1 probing phylloxera stage (Savoi et al., 2020).

Four other families from clan 3 (CYP6NZ, CYP6PA, CYP6PC and CYP6PD) were specifically found in *D. vitifoliae* but were absent from *M. persicae* and *A. pisum* and are derived from CYP6CY ancestor duplications. Interestingly, the scaffold 375 contained CYP6PA1 and CYP6PC1 together with four genes from the CYP6CY family (Suppl data Figure 3; data scaffold 375). These genes might be involved in host plant and feeding site selections. The DvCYP6CY family is reduced, with eight members annotated in *D. vitifoliae* compared to 16 in *A. pisum* and 17 in *M. persicae* (Mathers et al., 2017).. DvCYP6CYs showed high expression in RA forms, with CYP6CY25 having the lowest expression and CYP6CY26 the highest (Figure 2B). DvCYP6CY25 was the closest ortholog of the blooming CYP6CY family of *M. persicae* and *A. pisum* and grouped in a clade with eight *A. pisum* and three *M. persicae* CYP6CYs suggesting it was present in a common ancestor. The other CYP6CYs grouped in a single *D. vitifoliae* branch (Figure 2A). MpCYP6CY3 detoxifies the plant pyridine alkaloid, nicotine (Bass et al., 2013) and six genes from the CYP6CY family are involved in adaptive evolution to plant hosts in *Aphis glycine* (Bansal et al., 2014). CYP6CY genes specific to the *D. vitifoliae* genome might be involved in the detoxification of grape secondary metabolites like phenolic compounds (chlorogenic acid, quercetin, and tannins) together with phylloxera-specific CYP6PA, CYP6PC and CYP6NZ. CYP6PD1 is

expressed 100-times more in RA forms compared to GA (Figure 2B, Suppl data Table 2 and (Rispe et al., 2016)).

We annotated a new CYP family, CYP3806A, previously named CYP3373A (Rispe et al., 2020) and classified in CYP4 clade. CYP3806A1 is expressed 100-fold higher in RA forms than GA (Suppl data Table 2 ,Figure 2B). This new gene family shared a common ancestor with CYP4LR-LP-LS and CYP4CH families (Figure 2 A). CYP380B1 was the only 1:1 ortholog in *A. pisum* and *M. persicae* genomes from the CYP4 clade, and it is highly expressed in adult forms. CYP380B1 is highly expressed in the feeding L2-L3 larval stage compared to probing L1 stage and is up-regulated in phylloxera biotype C feeding on the rootstock Teleki 5C (Savoi et al., 2020). This gene could be linked to the manipulation of plant metabolism and hormones (cytokinins) by insects during sap feeding (Zhang et al., 2017). The CYP380C family has 11 members all blooming from CYP380C6 ancestor. Six CYP380C are clustered on two scaffolds (315 and 386) with three genes on each indicating recent duplication events. Seven CYP380C members (CYP380C22,23,24,26,28,29 and 36) had higher expression in RA compared to GA forms. CYP380C6 and C9 from green peach aphid are induced while feeding and are involved in aphid adaptation to indole-glucosinolate mediated plant defense (Ji et al., 2020). Their phylloxera ortholog, CYP380C36, is highly expressed in RA and is also up regulated in the probing stage (Savoi et al., 2020). This gene could be involved in phylloxera response to root derived compounds synthetized after phylloxera wounding (Du et al., 2009). We annotated three members of the CYP4G family in *D. vitifoliae* clustered on scaffold 379. Only one copy of this family, DvCYP4G194, has an ortholog in *M. persicae* and *A. pisum* (Figure 2A), and is involved in cuticular long-chain hydrocarbon synthesis (Chen et al., 2016, Feyereisen, 2020, Qiu et al., 2012). A DvCYP4G194 duplication produced two additional copies (CYP4G195 and CYP4G196). The three DvCYP4Gs showed the highest expression among all DvCYPs as is often seen in insects (Daborn et al., 2002, Feyereisen, 2020). CYP4G196 is highly expressed in the L2-3 form, whereas CYP4G194 and CYP4G195 have increased expression in L1 forms of phylloxera biotype A (Savoi et al., 2020). CYP4LQ1 and 2 cluster with CYP4CJ6,7and 8 as well as with the GSTomega1 and a chitin synthase (Suppl data Figure 4). All these clustered genes are highly expressed in adult forms except for CYP4LQ1 which is only expressed in RA. CYP4LQ1 and CYP4CJ6 are expressed in the L1-probing stage together with CYP4LN1, CYP4LP1, CYP4LR1, CYP4LS2 and CYP4CH4 (Savoi et al., 2020). In all inducer *Agrobacterium tumefaciens,* virH2, a P450, detoxifies phenolic compounds such as ferulic acid (Kalogeraki et al., 1999). These compounds also accumulate in root gall upon phylloxera attack (Du et al., 2009). DvCYPs expressed when L1 larvae are selecting host plants and feeding sites may reflect their implication in phenolic compounds detoxification.

CCE

Twenty genes encoding CCEs were retrieved from the *D. vitifoliae* genome, across thirteen scaffolds (see Suppl data Table 1 for gene position, exon number and orientation). Twelve sequences bearing a putative alpha/beta domain but not the CCE domain were discarded. With the exception of sequences encoding non-catalytic NLGs and Gliotactin, all other DvCCEs displayed the catalytic triad (Ser-His-Glu) with the serine-active site included in the conserved pentapeptide Gly-X-Ser-X-Gly (Claudianos et al., 1999) (Suppl data Table 3), suggesting that they could encode active enzymes. The total number of DvCCEs is much lower than the mean number of sequences found in other insect genomes (Table 1), with the exception of the body louse *Pediculus humanus* (17 genes (Ramsey et al., 2010) and the bee *A. mellifera* (24 genes (Claudianos et al., 2006)), known to exhibit a deficit in detoxification enzymes.

The neuro/developmental class comprises eight members in *D. vitifoliae*, including two AChE genes, three NLGs and one member of the glutactin and gliotactin families, respectively (Table 1). Phylogenetic analysis (Figure 4A) showed clear orthologous relationships for these genes between the four hemipteran species, confirming previous results (Schama et al., 2016, Ramsey et al., 2010).

In *D. vitifoliae*, three sequences belonging to the NLG clade have been isolated (DvCCE13,14,19), all of which possess hydrophobic transmembrane regions. DvCCE13 and 19 are more highly expressed in probing larvae, whereas DvitCCE14 is expressed in the L2-3 feeding stage (Savoi et al., 2020). The number of annotated NLGs differ depending on the species: one in *M. persicae,* up to ten in *Bemisia tabaci* (Xia et al., 2019), six in *B. mori* and four in *D. melanogaster* (reviewed in (Durand et al., 2017)). Overall, this neuro/developmental class is well-conserved amongst insects, as supported by several phylogenetic analyses comparing CCE genes from various insect orders, such as Hymenoptera (Oakeshott et al., 2010) (Claudianos et al., 2006), Lepidoptera (Yu et al., 2009) and Diptera (Oakeshott et al., 2010). DvCCE16 encodes a putative glutactin protein, but the remaining CCEs from this first class are expressed at low levels in *D. vitifoliae* adult stages (Figure 4B), as expected for genes mainly involved in cell adhesion during neural development. AChEs are the most studied enzymes from this class. They have conserved functions in insects with the hydrolysis of neurotransmitter acetylcholine. Like most insects, *D. vitifoliae* possesses two AChE genes, one predicted to be membrane-bound with a GPI anchor signal (DvCCE8=AChE1), the other to be secreted (DvCCE9=AchE2). Both DvCCE8 and 9 are expressed in L1 larvae (Savoi et al., 2020). Insect AChEs are known targets of carbamate and organophosphorus insecticides (Oakeshott et al., 2010). A point mutation that causes a single amino acid substitution (S341F) in the acyl pocket of AChE1 has been associated with insecticide resistance, first in *M. persicae* resistant clones (Nabeshima et al., 2003), then in other aphid species (reviewed in (Bass et al., 2014)) (Suppl data Figure 5). More recently, a F392W substitution has been observed in the AChE1 sequence from a Chinese *B. tabaci* chlorpyrifos resistant strain (Zhang et al., 2012). However, this mutation was not responsible for insecticide resistance, as it was also found in susceptible populations from the field. Interestingly, the DvCCE8 sequence isolated here also exhibits a tryptophan at the same position (Suppl data Figure 5). suggesting that this F392W substitution may be common amongst hemipterans.

D. vitifoliae appears to possess only two genes (DvCCE17, 18) encoding intracellular enzymes related to the detoxification/dietary class (Figure 4A). In *A. pisum,* and *M. persicae* only five or six sequences from this class were identified, and none were found in triatomines (Traverso et al., 2017). *R. prolixus* is an exception among hemipterans as it may possess 22 of these CCEs. However, their phylogenetic assignment was not well supported (Schama et al., 2016) and they mostly clustered into a *R. prolixus* specific group in our analysis, but again with low support values (Figure 4A). The low expansion of this CCE class within hemipterans is in marked contrast with other insect orders which generally retain more. (Table 1). Nevertheless, DvCCE17 and DvCCE18 are strongly expressed in both adult forms (Figure 4B), and DvCCE18 is upregulated in feeding larvae (Savoi et al., 2020), consistent with the detoxification of dietary or allelochemical compounds.

In *D. vitifoliae,* as in other hemipteran species, the low number of CCEs from the second class is counterbalanced by a diversification of hormone/pheromone processing CCEs. In sucking insects, the relative expansion of this class, which mainly includes secreted enzymes, may be useful for detoxification process in the gut or the salivary secretions that are pumped into the host (plant or animal) as they feed. Ten DvCCEs belonging to this third class were identified, comparable to the twelve sequences isolated in *M. persicae,* but still far from the diversity identified in other hemipterans (Table1). Eight of these clustered with *A. pisum and M. persicae* genes related to JHE and JHE-like enzymes. These eight sequences were located on only two scaffolds, suggesting duplication events. No ortholog for the *A. pisum* JHE (ACYPI007757; (Ishikawa et al., Schama et al., 2016) was found. Nevertheless, DvCCE2 and DvCCE10 both exhibit the "QSAG" motif which strongly correlated with insect JHE (Oakeshott et al., 2010) and both are predicted to be secreted proteins with active catalytic sites (Suppl data Table 3). DvCCE7 and 10 were predicted to be putative effector candidates, and were expressed in L1 larvae and L2-3 larvae, respectively (Savoi et al., 2020). Aphid CCEs from this JHE/JHE-like clade split into several sub-groups suggesting that that they may descend from an ancestral JHE but that some have gained new functions. Finally, two genes (DvCCE11 and DvCCE12) from this third class clustered within the β-esterase clade, which contains almost exclusively secreted enzymes. DvCCE12 is expressed in feeding larvae (Savoi et al., 2020). β-esterase

overexpression suggested a major mechanism of resistance to organophosphate and carbamate insecticides in hemipterans ((Field and Devonshire, 1998); review in (Bass et al., 2014)). These CCEs were also recently found to be involved in neonicotinoid resistance in *B. tabaci* (Xia et al., 2019). In addition, β-esterases have other biological functions, including reproduction and odorant processing (Chertemps et al., 2012, Chertemps et al., 2015, Richmond et al., 1980, Scott, 1986). In *D. vitifoliae*, the genes of this third class showed marked differences in expression between the two adult forms (Figure 4B). In particular, DvCCE1 and DvCCE2 showed high expression levels in RA compared to GA forms, whereas DvCCE11 is mostly predominant in GA-adult. All three DvCCEs exhibit higher expression in feeding phylloxera larvae (Savoi et al., 2020). These differences may reflect variations in exposure to allelochemicals, in relation to the distinct environments of these adult forms.

Phase II enzymes: UGT and GST

GSTs

In insect GSTs, the cytosolic class contains six subclasses (Delta, Epsilon, Omega, Sigma, Theta and Zeta) (Sheehan et al., 2001).The microsomal GSTs are very different in structure and origin but they catalyze similar reactions to the cytosolic GSTs (Toba and Aigaki, 2000). We annotated only 10 GST genes (see Suppl data Table 1 for gene position, exon number and orientation). This number is comparable to GST numbers found in other Hemipteran genomes (Table1) like *M. persicae* or *R. prolixus*, but lower than in *A. pisum* (Ramsey et al., 2010, Schama et al., 2016) and similar to the 8 genes identified in the *D. vitifoliae* transcriptome (Zhao et al., 2017). A low number of genes is often associated with reduced detoxification capabilities (Claudianos et al., 2006). Nevertheless, such low diversity is often observed in aphids and could be linked to specific adaptations to environmental conditions. The distribution of GST genes revealed classical duplication events, with genes belonging to the same class located in the same scaffold and in the same orientation. Patterns of inter-specific conservation and lineage-specific expansion of the gene family were observed (Figure 5A). The phylogenetic analysis enables unambiguous identification of *D. vitifoliae* GST classes. As in other aphids, we did not identify any epsilon GSTs, a class involved in insecticide resistance in other insects (Ding et al., 2003). This could suggest the recruitment of other GSTs in this process, like the insect specific delta class (Vontas et al., 2002) which is phylogenetically associated with epsilon GST, or the involvement of detoxification enzymes. In addition, the absence of GSTs from the zeta and unclassified class, both of which are involved in insecticide resistance in Lepidoptera species (Yamamoto et al., 2009, Yamamoto and Yamada, 2016), leads to a potential similar selection of detoxification capabilities in other classes of GSTs. Overall, the cytosolic DvGSTs *a*ppeared to be very closely related to the *M. persicae* repertoire, and could be associated with defense against plant secondary metabolites. GSTd2 is highly expressed in adult forms (Figure 5B). GSTs2 and 3, GSTd1 and GSTt1 displayed low expression in adult forms, and Savoi *et al.* reported higher expression of these genes in feeding larvae compared to probing larvae (Savoi et al., 2020). GSTs1 is expressed in RA and GA, and is more expressed in mobile probing L1 larvae than in feeding L2-3 larvae (Savoi et al., 2020). Overall, cytosolic GSTs are more expressed in RA adults where, in addition to detoxifying plant secondary metabolites, they could play an important role in protection against external factors like bacterial infections, temperature stress or entropic contaminants such as heavy metals or insecticides. Such functions have often been associated with increased expression following exposure to stress in aphids and various insects (Enayati et al., 2005, Gawande et al., 2014, Zhou et al., 2013). We identified three microsomal GSTs in *D. vitifoliae* genome, the highest number of mGSTs described so far in aphids. We found a highly conserved region (ERVRRAHLNDLENI) in all insect mGSTs analyzed (Suppl data Figure 6), indicating its potential importance as a functional domain. Microsomal class GST genes are involved in cell protection from oxidative damage and xenobiotics, thus this relatively high diversity of mGSTs could highlight an original stress response mechanism. While *D. vitifoliae*

MAPEGs are very conserved, their expression pattern is remarkably different: mGST1 and 2 are expressed at very low levels in adult forms but data obtained by Savoi *et al.* showed that mGST1 and 2 are more expressed in L1 larvae compared to L2-3 larvae (Savoi et al., 2020). Microsomal GST1 and 2 are also expressed at low levels in GA and RA, and might therefore be involved in the early phase of phylloxera-grapevine interaction, whereas mGST3, which is broadly expressed in all tissues and development stages, could be involved in detoxification of substrates accumulated during feeding (L2-3 larval stages) and adult phylloxera forms.

UGTs

The *D. vitifoliae* genome contains 35 putative UGT genes (Suppl data Table 1), which is similar to other aphids, particularly in *M. persicae* (38) and *A. pisum* (55), and comparable to that of *Aphis gossypii* (31) (Pan et al., 2018), and *Bemisia tabaci* (76) (Guo et al., 2020) and *Diaphorina citri* (17) (Tian et al., 2019) (Table 1). DvUGTs are distributed across 10 sub-families when compared to the curated UGTs repertoires from *M. persicae* and *A. pisum*. The phylogeny reveals the absence of the UGT50 family, which is usually highly conserved in holometabolous insects, a common feature with the UGTs of *A. pisum* and *M. persicae*, suggesting the recruitment of other candidate for its relative function. A major sub-family, UGT344, accounts for nearly half of the sequences identified, indicating that this clade should have potential functional diversification in *D. vitifoliae* (Figure 6A). Expansion of 10 genes of the 344N sub-family was found in the scaffold 572 cluster (Suppl data Figure 7). This expansion is associated with a wide range of expression patterns ranging from a near absence for UGT344N4-N6 and UGT344N2 in GA, to high specific expression for UGT344N3 in RA. UGT344N4 and UGT344M2 are strongly expressed in L2-3 forms, while UGT344N2, N3, N6 and N7 are more expressed in L1 forms. Interestingly, UGT344N10 is only expressed in biotype C L1 larvae. Such varied expression patterns could be related to various exogenous detoxification pathways, given that members of the 344 family are often associated with aphid insecticide resistance (Pan et al., 2018, Pan et al., 2019). The distribution of UGT genes over the identified scaffolds revealed further duplication events, with scaffold 424 and 572 accounting for almost 50% of the total gene number, suggesting rapid evolution of these families. Expression levels of genes present in the scaffold 424 cluster are also heterogeneous, with UGT349A2-A5 showing high expression in RA compared to GA and high expression in L2-3 forms while UGT349A4-A7 are expressed in biotype C L1 larvae. The same is true for the expression levels of the remaining UGT genes: almost no expression was detected for UGT343C5,350C2,349A4,351A3,349A6 in the two adult forms. In contrast, UGT329A1 and UGT350C1 were the highest expressed UGTs in both GA and RA forms, respectively (Figure 6B). Finally, UGT344F3 is the only UGT specifically expressed in biotype C L1 forms, whereas UGT344N1,339A3,343C4 are highly expressed in L1 forms in all biotypes studied. The varied expression patterns for UGTs might reflect a diversity of functions during phylloxera-grapevine interactions, but also multiple potential functions in cuticle tanning, pigmentation and even olfaction, as observed in other insect species (Bozzolan et al., 2014, Hopkins and Kramer, 1992).

Phase III enzymes: ATP-binding cassette transporters

ABC transporters are classified into eight different families (A to H) based on similarities in their ATP binding domain. A full transporter (FT) contains two cytosolic nucleotide-binding domains (NBDs) and two transmembrane domains (TMDs), whereas a half transporter (HT) possesses only one of each domain and needs to dimerize to form a functional transporter. The NBD is involved in ATP binding and hydrolysis. The TMD has 5-6 transmembrane segments and is responsible for substrate specificity.

D. vitifoliae genome hosts 67 ABC transporter genes, spread over 48 scaffolds. This total number is close to the 71 genes identified automatically in *A. pisum (International Aphid Genomics, 2010)* (Table 1) and is in the same range as the 55 ABC transporters of *B. tabaci* (Nicholson et al., 2015, Tian et al., 2017). However, a smaller number of ABC transporters has been identified in another recently

sequenced Hemiptera, *T. vaporariorum,* with 45 genes (Pym et al., 2019). ABCD, ABCE, ABCF subfamilies are well conserved across arthropods, whereas specific lineages showed a reduction (ABCA, ABCC) or an expansion (ABCG and ABCH) in their gene number in *D. vitifoliae*.

ABCA is limited to 4 members, similar to the number present in *D. noxia* (Nicholson et al., 2015). ABCAs are full transporters and are among the largest ABC transporters. In humans, they are involved in lipid transport (Wenzel et al., 2007), however this has not yet been demonstrated in insects. However, the Bt toxin receptor function was described and mutations in ABCA2 were shown to confer resistance to Cry2Ab toxin in *Helicoverpa armigera* and *H. punctigera* (Tay et al., 2015). In addition, a role in wing development has been suggested in *T. castaneum* (Broehan et al., 2013). DvABCA1 and DvABCA2 were highly expressed in GA and RA, while DvABCA4 was expressed in L1 probing larvae (Savoi et al., 2020) (Figure 7B).

ABCBs commonly refer to either P-glycoproteins (P-gps) or multi drug resistance proteins (MDR). DvABCBs group 2 FTs and 4 HTs. DvABCB1 FT shares orthologous relationships with *D. melanogaster* Mdr65 and *Manduca* sexta ABCB1, which is involved in drug efflux at the blood-brain barrier (BBB) (Murray et al., 1994). Furthermore, studies showed that Mdr65 RNAi knock-down *Drosophila* are more sensitive to nine insecticides from different chemical classes (Sun et al., 2017a). DmMdr65 has also been suggested to play a major role in protection against plant toxins such as cardenolides (Groen et al., 2017), a role also suggested for ABCB in Lepidoptera (Petschenka et al., 2013) and in Coleoptera (Kowalski et al., 2020). DvABCB6 exhibits a mitochondrial-addressing domain, and human mitochondrial ABCBs have roles in biogenesis of cytosolic iron-sulfur clusters, heme biosynthesis and prevention of oxidative stress (Schaedler et al., 2015). Given their similarities, mitochondrial ABCBs might have a conserved role from humans to arthropods. Expression levels of all DvABCBs are relatively high in the adult forms, with only DvABCB3 showing a very low expression level (Figure 7B). Expression levels of DvABCBs were higher in L2-3 feeding larvae compared to L1 probing larvae, except for DVABCB2 (Savoi et al., 2020).

ABCCs are also named multidrug-resistance associated proteins (MRPs) for their role in drug extrusion. This subfamily has fewer members in *D. vitifoliae,* with only five genes, which is less than *A. mellifera* but similar to *Laodelphax striatellus* (Sun et al., 2017b). This is the smallest number observed in the genomes available to date. This lineage-specific reduction in ABCCs is also observed in two other Hemiptera, *B. tabaci* and *Cimex lectularius,* with only six genes coding for ABCC (Tian et al., 2017). At least two other functions have been identified for humans ABCCs in addition to MRPs: a sulfonylurea receptor (SUR) and a cystic fibrosis transmembrane conductance regulator (CFTR). ABCs with these different functions were identified in insects. The adult expressed DvABCC1, and DvABCC4 are MRPs (Figure 7B). DvABCC2-3 share orthology with human ABCC4 and ABCC7/CFTR. DvABCC3 is also highly expressed in adults (Figure 7B). DvABCC5 is a SUR ortholog and is the only DvABCC member detected with higher expression in L1 larvae compared to L2-3 larvae (Savoi et al., 2020).

The subfamily **ABCD** is composed of HTs that need to homo- or hetero-dimerize to be functional. Three members have been identified in *D. vitifoliae* genome, which is identical to *P. xylostella, Danaus plexippus* and *D. pulex* (Qi et al., 2016, Sturm et al., 2009). The high sequence identity found in ABCDs from humans to arthropods suggests conserved functions. Human ABCDs are expressed at the peroxisomal membrane and are involved in fatty acid and fatty acyl-CoA transport into the peroxisome (Morita and Imanaka, 2012). In accordance with this putative role in insects, all DvABCDs are highly expressed in adult forms (Figure 7B).

ABCE1 and **ABCF1-3** are highly conserved in arthropods and share a human ortholog suggesting conserved function. Both of these subfamilies contain only two NBDs and lack TMDs which abolishes transporter function. ABCE is involved in ribosome biogenesis and translation regulation (Barthelme et al., 2011), whereas ABCFs have functions in translation regulation only. ABCE and ABCFs are highly expressed during all stages of arthropod development which is consistent with a function in

translation regulation (Broehan et al., 2013, Dermauw et al., 2013, Qi et al., 2016) and is in agreement with our expression data (Figure 7B).

D. vitifoliae possesses 22 genes coding for **ABCG**, a number very close to other piercing-sucking arthropods (Tian et al., 2017) and higher than chewing insects, which usually have around 15 members. This specific expansion may be due to successive duplications, as we found four scaffolds with more than two ABCGs (scaffold31-40-88-213). ABCGs are historically the most well described ABC transporters. *White* was the first identified in *D. melanogaster* with a role in eye pigmentation (Morgan, 1910), followed by *brown* and *scarlet*, which are also involved in eye-color. In addition to their roles as pigment precursor transporters, they have functions in courtship behavior (Zhang and Odenwald, 1995), transport of biogenic amines (Borycz et al., 2008) and uptake of uric acid (Tatematsu et al., 2011). One *white* ortholog, DvABCG17, was identified in the *D. vitifoliae* genome while DvABCG18, DvABCG19, and DvABCG20 are paralogs of *scarlet.* DvABCG16 is the ortholog of another highly conserved ABCG gene in insects, DmE23. This ABCG transporter can be induced by the hormone 20-hydroxy-ecdysone and thus modulates ecdysone responses (Hock et al., 2000). ABCGs are also involved in lipid transport from the epidermis to the cuticle (Broehan et al., 2013). Our data revealed that expression patterns between the 22 ABCG members are diverse (Figure 7B), with low or no expression of ABCG20, 21 and 22, as confirmed by (Savoi et al., 2020), whereas ABCG1 is one of the most expressed ABC transporters in *D. vitifoliae*. Scarlet (DvABCG18) is highly expressed in GA, but the opposite expression is seen for DvABCG14. DvABCG18 is also more expressed in probing forms compared to feeding forms (Savoi et al., 2020).

The **ABCH** subfamily is restricted to arthropods and zebrafish (Popovic et al., 2010) and has not been found in mammals, plants or fungi (Dean et al., 2001, Kovalchuk and Driessen, 2010, Verrier et al., 2008). In *D. vitifoliae*, ABCH consists of 23 genes corresponding to one third of the total ABC transporter genes and thus constitutes the largest subfamily. Several genes are present in cluster: five genes on scaffold 184 (Suppl data Figure 1), while scaffolds 36 (Suppl data Figure 8) and 129 (Suppl data Figure 9) carry four genes each. ABCHs on scaffold 36 have a conserved 15-exon organization and high protein identity, suggesting recent tandem duplications. Interestingly, the genes surrounding this cluster are six predicted effector genes (Suppl data Figure 9). Such extensive expansion of the DvABCH subfamily is only observed in *T. urticae (Dermauw et al., 2013)*. Some members of this subfamily have a role in cuticle barrier construction via lipid transport as reported in *Locusta migratoria* and *T. castaneum* studies (Broehan et al., 2013, Yu et al., 2017). In *D. melanogaster* Oskyddad (Osy) and Snustorr (Snu) are required to build the cuticular desiccation barrier (Wang et al., 2020, Zuber et al., 2018). The *D. vitifoliae* orthologs of these genes are DvABCH1 and DvABCH2, respectively, and they are highly expressed in adult forms (Figure 7B), which is in accordance with their expected function. The ABCH transporter family displays different expression patterns in RA and GA. For example, DvABCH16 is higher in GA than RA (Figure 7B) and more expressed in L1 than in L2-3 larvae (Savoi et al., 2020). Mite ABCH genes showed differential expression after host plant transfer or xenobiotic exposure, suggesting their potential involvement in detoxification mechanisms (Dermauw et al., 2013). This might also apply to *D. vitifoliae* ABCHs as we observed differential expression patterns between the two adult forms with root and leaf environments, and between the probing and feeding larvae.

CONCLUSIONS

D. vitifoliae is a xylem-sucking aphid that monophagously feeds on grapevines. We analyzed the detoxification gene repertoire of phylloxera. Genes coding for phase I (66 CYPs, 20 CCEs), phase II (35 UGTs, 11 GSTs) and phase III (67 ABC transporters) enzymes were found in the *D. vitifoliae* genome and we are able to make predictions about their physiological roles, according to both their

expression patterns and described functions from other models. The Halloween genes are involved in ecdysteroid synthesis and regulation, and DvCCE2 and 10 are probably JHE enzymes. DvABCG16 is orthologous to an ABCG transporter modulating ecdysone response. DvCYP303A1 and DvCYP4G are involved in cuticular hydrocarbon synthesis. DvCCEs from the neuro/developmental class are crucial for nervous system development. DvABCE1 are most probably involved ribosome biogenesis and translation regulation. While feeding on a plant, the insect is reprogramming leaf and root development toward galls by manipulating primary and secondary metabolism. We found expansions of several sub-families including DvCYP6CZ (four members), DvCYP380C (eleven), microsomal DvGST (three), DvUGT344N (ten members) and DvABCH (23). Members of these families could be involved in xenobiotic detoxifications. DvCYP3806A1 was only found in phylloxera and is highly expressed in RA. DvCYP6PD1 expression is also 100-fold more in RA than GA. Both genes might have a major role in root metabolite detoxification. DvCYP380B1, a rare 1:1 ortholog between *A. pisum*, *M. persicae* and *D. vitifoliae*, is highly expressed in feeding L2-3 and up-regulated in insects feeding on resistant rootstock. DvCYP4LQ1 and DvCYP4CJ6 might detoxify phenolic compounds induced during insect probing. DvCCE7 and 10 were predicted to be putative effector candidates by Savoi *et al.* (Savoi et al., 2020) and our phylogenetic data assigned these two CCEs as secreted enzymes from class III, which are often associated with detoxification processes. Microsomal GST1 and 2 might be involved in early phases of phylloxera-grapevine interaction, whereas mGST3 could be involved in detoxification of substrates accumulated during L2-3 feeding and in adult forms. We found that DvABCH1 and H2 genes are orthologs of genes involved in cuticular lipid transport and possibly xenobiotic excretion. Finally, we found several loci where detoxification families were in the vicinity of effectors and developmental genes. Our work provides a list of candidate genes for future functional investigation aimed at elucidating phylloxera adaptation to grapevine. We have highlighted the main characteristics of these detoxification families in *D. vitifoliae* with a specific focus on adaptation to host plant secondary metabolites and insect endogenous compounds.

Experimental procedures

Divergent time estimation

We used TimeTree, a knowledge-base for information on the tree-of-life and its evolutionary time scale (Kumar et al., 2017) to estimate divergent time between *D. vitifoliae*, *A. pisum*, *M. persicae* and *R. prolixus*.

Transcriptome data

Transcriptome data from adult forms of *D. vitifoliae* that feed respectively on leaves (GA) and roots (RA) was published by Rispe et al. 2016 (project accession: PRJNA294954). We mapped these data on the *D. vitifoliae* genome v3.1 using OGS3.2 annotations (Rispe et al., 2020). Hisat2 and transcript abundance was subsequently quantified using RSEM to obtain a "transcript per million" estimation. We screened these data with our detoxification gene annotation lists (Suppl data Table 2), and used the heatmap.2 function from the R gplots package with the Euclidean distance and the complete hierarchical clustering methods to obtain our heatmap figures.

Gene annotations and phylogenetic analysis

We used described sets of Hemiptera P450, CCE GSTs, UGTs and ABC transporter proteins to search the *D. vitifoliae* genome, Pcf7-strain v3.1 (Rispe et al., 2020)., by TBLASTN using Galaxy (Giardine et al., 2005). All gene models were manually validated or corrected in WebApollo based on homology

with other Hemipteran sequences, and on alignment with RNAseq data, when available. Alternatively, a direct keyword query search was used against the AphidBASE website (http://bipaa.genouest.org/is/aphidbase/). The classification of deduced proteins and their integrity were verified using BlastP against the non-redundant (nr) GenBank database. When genes were suspected to split in different scaffolds, protein sequences were merged for further analyses. Genes were also searched by TBLASTN against the whole genome assembly using CCE, CYP, UGT and GST proteins sequences from *N. vitripennis*, *R. prolixus*, *A. pisum* and *M. persicae* collected from the latest NCBI release. ABC transporters genes from *D. vitifolia* genome were searched by TBLASTN using ABC transporter proteins sequences from *D. melanogaster* and *A. mellifera*.

Amino acid sequences were aligned using MAFFT (using L-INS-i option) (Katoh et al., 2019) with different gene families members from *Myzus persicae*, *Rhodnius prolixus* and *Acyrthosiphon pisum* (Ramsey et al., 2010, Schama et al., 2016). Phylogenetic trees were constructed using PhyML (Guindon et al., 2010) based on the LG substitution model (see Suppl data Table 4) as determined by the SMS server (Lefort et al., 2017) using Nearest Neighbour Interchange (NNI). Branch supports were estimated by a Bayesian-like transformation of aLRT (aBayes) (Anisimova et al., 2011). A dendrogram was created and colored using FigTree software (http://tree.bio.ed.ac.uk/software/figtree/). Protein CYP sequences were send to D. Nelson for name attribution.

Acknowledgements

Funding for *Daktulosphaira vitifoliae* clone Pcf genomic sequencing was provided by Inra (AIP Bioressources) and BGI Biotech in the frame of i5k initiative. Parts of the transcriptomic resources were obtained within the 1KITE projects (Bernhard Misof, Bonn, Germany). We are grateful to Dr David Nelson for naming CYP. We would like to thank Dr C Rispe and F Legeai for giving access to their GA and RA transcriptomic data. We also thank Dr C Coustau for constructive discussions on the manuscript. The authors would like to thank Dr Abby Cuttriss (UCA-Office of International Scientific Visibility)

Figures legends

Figure 1: *D. vitifoliae* life cycle

Life cycle drawing was adapted from Annu. Rev. Entomol 2001, 46:387-412 and Entomologia experimentalis et applicata. 2009 vol:131 (1) pp:1-10. Gall corresponds to the grey form surrounding by an orange line. Sexual forms are in blue.

Figure 2: Phylogeny and expression heatmap for CYP family members

Panel A: Phylogeny of CYP found in *D. vitifoliae* (Dvit in red), *A. pisum* (Apis in green), *M. persicae* (Mper in purple) and *R. prolixus* (Rpro in blue). The DvCYP nomenclature was given by D Nelson. The other CYP names were taken from (Feyereisen, 2011a, Grbic et al., 2011, Dermauw et al., 2020). Colored lines correspond to branches with species using the same colors as for the CYP names. Numbers on the tree correspond to bootstrap values above 0.8. CYP clans were colored pink for the mitochondrial clan, purple for clan2, yellow for clan3 and green for clan4. Scale is given in the middle of the tree.

Panel B: Heatmap of expression levels for DvCYP in gallicole and radicicole adults. Color scale is given with more highly expressed DvCYPs in red and lower expressed DvCYPs in blue. Hierarchical clustering is given on the left side of the heatmap.

Figure 3 Ecdysteroid biosynthetic pathway associated with RA and GA expression levels

Dotted line is representing putative steps as part of the 'Black box' in the ecdysteroid pathway (Schumann et al., 2018a). The blue box shows gene expression levels in the radicicole adult (RA, dotted line) and in the gallicole adult (GA, plain line). These values were calculated using log2 of counts per million.

Figure 4: Phylogeny and expression heatmap for CCE family members

Panel A: Phylogeny of CCEs found in *D. vitifoliae* (Dvit in red), *A. pisum* (ACYP in green), *M. persicae* (Mper in purple) and *R. prolixus* (RPR in blue). Colored lines correspond to branches with species using the same colors code for the CCE names. Numbers on the tree correspond to bootstrap values above 0.8. CCE clades were colored with blue for pheromone/hormone processing class, light green for dietary class, pink for Nlg (L) and Glio (K) classes, yellow for AchE (J) class. Scale is given in the middle of the tree.

Panel B: Heatmap of expression level for DvCCEs in gallicole and radicicole adults. The color scale is given with more highly expressed DvCCEs in red and lower expressed DvCCEs in blue. Hierarchical clustering is given on the left side of the heatmap.

Figure 5: Phylogeny and expression heatmap for GST family members

Panel A: Phylogeny of GST found in *D. vitifoliae* (Dvit in red), *A. pisum* (Apis in green), *M. persicae* (Mper in purple) and *R. prolixus* (Rpro in blue). Colored lines correspond to branches with species using the same color code as for the CCE names. Numbers on the tree correspond to bootstrap values above 0.8. GST clades were colored with blue for MAPEG class, green for Sigma class, orange for Omega class, yellow for Theta class and pink for Delta class. Scale is given in the middle of the tree.

Panel B: Heatmap of expression level for DvGST in gallicole and radicicole adults. The color scale is given with more highly expressed DvGSTs in red and lower expressed DvGSTs in blue. Hierarchical clustering is given on the left side of the heatmap.

Figure 6: Phylogeny and expression heatmap for UGT family members

Panel A: Phylogeny of UGT found in *D. vitifoliae* (Dvit in red), *A. pisum* (Apis in green), *M. persicae* (Mper in purple) and *R. prolixus* (Rpro in blue). Colored lines correspond to branches with species using the same color code as for the UGT names. Numbers on the tree correspond to bootstrap values above 0.8. The UGT clades are colored with green for UGT329 and UGT343, pink for UGT348 and UGT350, blue for UGT330 and UGT349, purple for UGT339 and UGT342, and yellow for UGT344 and UGT341. Scale is given in the middle of the tree.

Panel B: Heatmap of expression levels for DvUGT in gallicole and radicicole adults. The color scale is given with more highly expressed DvUGTs in red and lower expressed DvUGTs in blue. Hierarchical clustering is given on the left side of the heatmap.

Figure 7: Phylogeny and expression heatmap for ABC transporter family members

Panel A: Phylogeny of ABC found in *D. vitifoliae*. Numbers on the tree correspond to bootstrap values above 0.8. ABC transporter clades are colored with purple for ABCC, orange for ABCD, light green for

ABCF, pink for ABCH, dark green for ABCG and yellow for ABCA. Scale is given in the middle of the tree.

Panel B: Heatmap of expression levels for DvABC in gallicole and radicicole adults. The color scale is given with more highly expressed DvABCs in red and lower expressed DvABCs in blue. Hierarchical clustering is given on the left side of the heatmap.

Table 1: Comparison of detoxification gene numbers in annotated insect species

GST, UGT, CCE, ABC transporter and CYP numbers from annotated genomes are compiled in this table. In addition to *D. vitifoliae,* the table contains *Acyrthosiphon pisum, Rhodnius prolixus, Bemisia tabaci, Myzus persicae,* and *Trialeurodes vaporariorum.*

References for data included in this table: *Bemisia tabaci* (Chen et al 2016 BMC biology 14(1)pp:110); *A. pisum* UGT sequences were reanalyzed based on the latest genome releases (AphidBase). Numbers in brackets denote number previously described UGTs in (Ramsey, Rider et al. 2010, Schama, Pedrini et al. 2016);) CYP numbers for *A. pisum* (Feyereisen R, 2011) and *M persicae* (Dermauw et al 2020). *:Ramsey et al, 2010, number based on EST data. ** *Acyrthosiphon pisum*, ABC transporter numbers obtained by automatic analysis. CCE data from *B. tabaci* (Xia et al, 2019, number corrected compared to Chen et al, 2016: 51 CCE); CCE data from *R. prolixus* from Schama et al, 2016 but assignment to clades were modified according to our phylogenetic analysis (Schama et al, 2016: 22 class I and 9 class 2); *Trialeurodes vaporariorum* (Pym A. et al 2019 BMC Genomics).

Supplementary data Figure 1: Gene organization and expression levels on scaffold 184

Scaffold184 carrying CYPs, effectors, ABCs, glutamate receptor and developmental genes in cluster. Genomic scale is given in base pairs (bp). Grey arrows correspond to ABC transporter genes, blue arrows to CYPs and black arrows to other genes. Expression levels in gallicole adult (GA) and radicicole adult (RA) are given in log2 of count per million. Numbers corresponding to expression levels are given in maroon boxes with a plain line for GA and dotted line for RA.

Supplementary data Figure 2: Gene organization and expression levels on scaffold 156

Scaffold156 carrying CYPs (CYP6NZ1, CYP6CY25, CYP6CZ2 and CYP6CZ fragment), sodium channel, farnesoic acid O-methyl transferase and carbonic anhydrase genes in cluster. Genomic scale is given in base pairs (bp). Blue arrows to CYPs and black arrows to other genes. Dashed arrow represents an incomplete gene sequence. Expression levels in gallicole adult (GA) and radicicole adult (RA) are given in log2 of count per million. Numbers corresponding to expression levels are given in maroon boxes with a plain line for GA and dotted line for RA.

Supplementary data Figure 3: Gene organization and expression levels on scaffold 375

Panel A: Scaffold 375 carrying six CYPs (CYP6CY67, CYPCY26, CYP6CY66, CYP6PC1, CYP6CY28, and CYP6PA1), in cluster. Genomic scale is given in base pairs (bp). Exon/intron gene representation is given in the arrow of each gene. Expression levels in gallicole adult (GA) and radicicole adult (RA) are given in log2 of count per million. Numbers corresponding to expression levels are given in maroon boxes with a plain line for GA and dotted line for RA. CYP6CY66 was previously named CYP6PB1. CYP6CY67 is a pseudogene (previously named CYP6PB2). No good estimation of expression was possible for CYP6CY67 and CYP6CY26 as they were considered to be a single gene in expression analysis.

Panel B: Phylogenetic tree extracted from the CYP family phylogenetic tree showing the eight members of CYP6CY (light blue), CYP6PA1 and CYP6NZ1 (in black), the two CYP6PCs (in grey) and two CYP6PDs (dark blue).

Supplementary data Figure 4: Gene organization and expression levels on scaffold 89

Scaffold 89 carrying five CYPs (CYP4LQ1 and 2, CYP4CJ6-7 and 8), a chitin synthase and a GSTomega1 in cluster. Genomic scale is given in base pairs (bp). CYPs are marked with blue arrows and other genes with black arrows. Expression levels in gallicole adult (GA) and radicicole adult (RA) are given in log2 of count per million. Numbers corresponding to expression levels are given in maroon boxes with a plain line for GA and dotted line for RA.

Supplementary data Figure 5: Amino acid alignment of AChE1 and AChE2 sequences from aphids and other insects

In bold: the amino acid where a substitution (F->W) is observed in *B. tabaci* clones that are resistant to clorpyrifos or where a substitution (S->F) is observed in *M. persicae* clones resistant to pirimicarb.
References of AChE1 sequences: *Bemisia tabaci* (ABV45413.1); *Myzus persicae* (AY147797); *Melanaphis sacchari* (XP_025206860.1); *Acyrtophison pisum* (ACYPI009886); *Aphis gossypii* (AJ748114); *Aphis craccivora* (KAF0771168.1); *Aphis glycines* (KAE9530899.1); *Rhodnius prolixus* (RPRC000482-PA). References of AChE2 sequences: *Bemisia tabaci* (ABV45415.1); *Myzus persicae* (CAE11220.1), *Acyrthosiphon pisum* (ACYPI009533); *Rhodnius prolixus* (RPRC003013; *Drosophila melanogaster* (X05893); *Lucilia cuprina* (U88631); and *Apis mellifera* (AF213012).

Supplementary data Figure 6: Microsomal GST proteins

Amino acid comparison of microsomal GST proteins from *D. vitifoliae* (Dvit), *M. persicae* (Mper), *R. prolixus* (Rpro), *S. furcifera* (Sfur) and *A. pisum* (Apis). The first line corresponds to the sequence Logo (conserved and most probable amino acids). The second line corresponds to identity in the sequence at each position. Green indicates complete identity and red indicates poor conservation of amino acid at that position. 11 MAPEG sequences were aligned. In the following order: Apis_MAPEG1, MperMAPEG1, Dvit_MGST1, Dvit_MGST2, Sfur_MAPEG1, Sfur_MAPEG2, Rpro_MAPEG1, Apis_MAPEG2, Mper_MAPEG2, and Dvit_MGST3.

Supplementary data Figure 7: Gene organization and expression levels on scaffold 572

Scaffold 572 carrying nine UGT344N (UGT344N2-3-4-6-7-8-9-10) with black arrows and UGT344M2 with blue arrow, in cluster. Genomic scale is given in base pairs (bp). Expression levels in gallicole adult (GA) and radicicole adult (RA) are given in log2 of count per million. Numbers corresponding to expression levels are given in maroon boxes with a plain line for GA and dotted line for RA. ND: not detected.

Supplementary data Figure 8: Gene organization and expression levels on scaffold 36

Scaffold 36 carrying four ABC transporters (black arrow) clustered with six effectors (blue arrow). Genomic scale is given in base pairs (bp). Expression levels in gallicole adult (GA) and radicicole adult (RA) are given in log2 of count per million. Numbers corresponding to expression levels are given in maroon boxes with a plain line for GA and dotted line for RA. ND: not detected.

Supplementary data Figure 9: Gene organization and expression levels on scaffold 129

Scaffold 129 carrying four ABC transporters (black arrow) clustered with one effector, three RING genes and groucho gene (blue arrows). Genomic scale is given in base pairs (bp). Expression levels in gallicole adult (GA) and radicicole adult (RA) are given in log2 of count per million. Numbers corresponding to expression levels are given in maroon boxes with a plain line for GA and dotted line for RA.

Supplementary Table 1: Detoxification genes position on *D vitifoliae* genome

Complete data set for each detoxification gene annotated on the genome of *D. vitifoliae*. In each column: scaffold number; position or transcript name; strand column describing the orientation of the gene of the scaffold; size indicating the size in amino-acid of the protein; exon column giving the number of exons; detox family column attributing the gene to one of the detoxification family (CYP, CCE, GST, UGT or ABC transporter); name_ID column presenting the unique identity of the gene; classification column indicating clan or class associated with the gene; name column giving the official name of the gene; and comments column listing additional gene information.

Supplementary Table 2: Expression data of detoxification genes for GA and RA

RNAseq data from GA and RA samples were analyzed for our annotated detoxification genes. GA and RA samples in duplicate were sequences, counts per million are given in this table. We calculated the mean and transformed the value in log2 of counts per million.

Supplementary Table 3: Summary of CCE specific characteristics

All DvCCEs were classified and analyzed in terms of the composition of their catalytic triad, the presence of a signal peptide or other domains and their subcellular localization.

Supplementary Table 4: Summary of model use for phylogenetic studies of detoxification families

Supplementary Table 5: Fasta file containing CYPs, UGTs, GSTs and ABC transporters amino acid sequences

Bibliography

ANISIMOVA, M., GIL, M., DUFAYARD, J.-F., DESSIMOZ, C. & GASCUEL, O. 2011. Survey of Branch Support Methods Demonstrates Accuracy, Power, and Robustness of Fast Likelihood-based Approximation Schemes. *Systematic Biology,* 60**,** 685-699.

BANSAL, R., MIAN, M. A., MITTAPALLI, O. & MICHEL, A. P. 2014. RNA-Seq reveals a xenobiotic stress response in the soybean aphid, Aphis glycines, when fed aphid-resistant soybean. *BMC Genomics,* 15**,** 972.

BARTHELME, D., DINKELAKER, S., ALBERS, S.-V., LONDEI, P., ERMLER, U. & TAMPÉ, R. 2011. Ribosome recycling depends on a mechanistic link between the FeS cluster domain and a conformational switch of the twin-ATPase ABCE1. *Proceedings of the National Academy of Sciences,* 108**,** 3228-3233.

BASS, C., PUINEAN, A. M., ZIMMER, C. T., DENHOLM, I., FIELD, L. M., FOSTER, S. P., GUTBROD, O., NAUEN, R., SLATER, R. & WILLIAMSON, M. S. 2014. The evolution of insecticide resistance in the peach potato aphid, Myzus persicae. *Insect Biochem Mol Biol,* 51**,** 41-51.

BASS, C., ZIMMER, C. T., RIVERON, J. M., WILDING, C. S., WONDJI, C. S., KAUSSMANN, M., FIELD, L. M., WILLIAMSON, M. S. & NAUEN, R. 2013. Gene amplification and microsatellite polymorphism underlie a recent insect host shift. *Proc Natl Acad Sci U S A,* 110**,** 19460-5.

BENHEIM, D., ROCHFORT, S., EZERNIEKS, V., POWELL, K. S., KOROSI, G. A., ROBERTSON, E. & POTTER, I. D. 2011. Early detection of grape phylloxera (Daktulosphaira vitifoliae Fitch) infestation through identification of chemical biomarkers. . *Acta Horticulturae,* 904**,** 17-24.

BODY, M. J. A., APPEL, H. M., EDGER, P. P. & SCHULTZ, J. C. 2019. A gall-forming insect manipulates hostplant phytohormone synthesis, concentrations, and signaling. *bioRxiv***,** 658823.

BORYCZ, J., BORYCZ, J. A., KUBÓW, A., LLOYD, V. & MEINERTZHAGEN, I. A. 2008. *Drosophila* ABC transporter mutants *white, brown* and *scarlet* have altered contents and distribution of biogenic amines in the brain. *Journal of Experimental Biology,* 211**,** 3454.

BOZZOLAN, F., SIAUSSAT, D., MARIA, A., DURAND, N., POTTIER, M. A., CHERTEMPS, T. & MAÏBÈCHE-COISNE, M. 2014. Antennal uridine diphosphate (UDP)-glycosyltransferases in a pest insect: diversity and putative function in odorant and xenobiotics clearance. *Insect Molecular Biology,* 23**,** 539-549.

BROEHAN, G., KROEGER, T., LORENZEN, M. & MERZENDORFER, H. 2013. Functional analysis of the ATP-binding cassette (ABC) transporter gene family of Tribolium castaneum. *BMC Genomics,* 14**,** 6.

CHEN, W., HASEGAWA, D. K., KAUR, N., KLIOT, A., PINHEIRO, P. V., LUAN, J., STENSMYR, M. C., ZHENG, Y., LIU, W., SUN, H., XU, Y., LUO, Y., KRUSE, A., YANG, X., KONTSEDALOV, S., LEBEDEV, G., FISHER, T. W., NELSON, D. R., HUNTER, W. B., BROWN, J. K., JANDER, G., CILIA, M., DOUGLAS, A. E., GHANIM, M., SIMMONS, A. M., WINTERMANTEL, W. M., LING, K. S. & FEI, Z. 2016. The draft genome of whitefly Bemisia tabaci MEAM1, a global crop pest, provides novel insights into virus transmission, host adaptation, and insecticide resistance. *BMC Biol,* 14**,** 110.

CHERTEMPS, T., FRANCOIS, A., DURAND, N., ROSELL, G., DEKKER, T., LUCAS, P. & MAIBECHE-COISNE, M. 2012. A carboxylesterase, Esterase-6, modulates sensory physiological and behavioral response dynamics to pheromone in Drosophila. *BMC Biol,* 10**,** 56.

CHERTEMPS, T., YOUNUS, F., STEINER, C., DURAND, N., COPPIN, C. W., PANDEY, G., OAKESHOTT, J. G. & MAIBECHE, M. 2015. An antennal carboxylesterase from Drosophila melanogaster, esterase 6, is a candidate odorant-degrading enzyme toward food odorants. *Front Physiol,* 6**,** 315.

CLAUDIANOS, C., RANSON, H., JOHNSON, R. M., BISWAS, S., SCHULER, M. A., BERENBAUM, M. R., FEYEREISEN, R. & OAKESHOTT, J. G. 2006. A deficit of detoxification enzymes: pesticide sensitivity and environmental response in the honeybee. *Insect Mol Biol,* 15**,** 615-36.

CLAUDIANOS, C., RUSSELL, R. J. & OAKESHOTT, J. G. 1999. The same amino acid substitution in orthologous esterases confers organophosphate resistance on the house fly and a blowfly. *Insect Biochem Mol Biol,* 29**,** 675-86.

DABORN, P. J., YEN, J. L., BOGWITZ, M. R., LE GOFF, G., FEIL, E., JEFFERS, S., TIJET, N., PERRY, T., HECKEL, D., BATTERHAM, P., FEYEREISEN, R., WILSON, T. G. & FFRENCH-CONSTANT, R. H. 2002. A single p450 allele associated with insecticide resistance in Drosophila. *Science,* 297**,** 2253-6.

DEAN, M., RZHETSKY A FAU - ALLIKMETS, R. & ALLIKMETS, R. 2001. The human ATP-binding cassette (ABC) transporter superfamily. *Genome Res.,* 11.

DENISOVA, T. V. 1965. The phenolic comlex of vine roots infested by phylloxera as a factor in resistance. *Vestnik Selskokhoziaistvennoi Nauki,* 10**,** 114-118.

DERMAUW, W., OSBORNE, E. J., CLARK, R. M., GRBIC, M., TIRRY, L. & VAN LEEUWEN, T. 2013. A burst of ABC genes in the genome of the polyphagous spider mite Tetranychus urticae. *BMC Genomics,* 14**,** 317.

DERMAUW, W., PYM, A., BASS, C., VAN LEEUWEN, T. & FEYEREISEN, R. 2018. Does host plant adaptation lead to pesticide resistance in generalist herbivores? *Curr Opin Insect Sci,* 26**,** 25-33.

DERMAUW, W., VAN LEEUWEN, T. & FEYEREISEN, R. 2020. Diversity and evolution of the P450 family in arthropods. *Insect Biochemistry and Molecular Biology***,** 103490.

DING, Y., ORTELLI, F., ROSSITER, L. C., HEMINGWAY, J. & RANSON, H. 2003. The Anopheles gambiae glutathione transferase supergene family: annotation, phylogeny and expression profiles. *BMC Genomics,* 4**,** 35.

DU, Y., ZHENG, Q., ZHAI, H., JIANG, E. & WANG, Z. 2009. Selectivity of Phylloxera viticola Fitch (Homoptera: Phylloxeridae) to grape with different resistance and the identification of grape root volatiles. *Acta Entomologica Sinica,* 52**,** 537-543.

DURAND, N., CHERTEMPS, T., BOZZOLAN, F. & MAIBECHE, M. 2017. Expression and modulation of neuroligin and neurexin in the olfactory organ of the cotton leaf worm Spodoptera littoralis. *Insect Sci,* 24**,** 210-221.

DÜRING, H. 1999. HIGH LIGHT AND WATER STRESS IN GRAPEVINES: PHOTOINHIBITION AND PHOTOPROTECTION. *Acta Horticulturae,* 493**,** 45-54.

EITLE, M. W., CARGNONI, M., ACAR, A., CRESPO MARTINEZ, S., FAILLA, O., KAUL, H.-P., GRIESSER, M. & FORNECK, A. 2017. Phylloxeration effects on the sink activity and assimilation rate in phylloxera (Daktulosphaira vitifoliae Fitch) infested grapevines (Vitis spp.). *Acta Horticulturae,* 1188**,** 291-298.

ENAYATI, A. A., RANSON, H. & HEMINGWAY, J. 2005. Insect glutathione transferases and insecticide resistance. *Insect Mol. Biol.,* 14**,** 3-8.

FEYEREISEN, R. 2011a. Arthropod CYPomes illustrate the tempo and mode in P450 evolution. *Biochimica et Biophysica Acta (BBA) - Proteins & Proteomics,* 1814**,** 19-28.

FEYEREISEN, R. 2011b. Arthropod CYPomes illustrate the tempo and mode in P450 evolution. *Biochim Biophys Acta,* 1814**,** 19-28.

FEYEREISEN, R. 2012. 8 - Insect CYP Genes and P450 Enzymes. *In:* GILBERT, L. I. (ed.) *Insect Molecular Biology and Biochemistry.* San Diego: Academic Press.

FEYEREISEN, R. 2020. Origin and evolution of the CYP4G subfamily in insects, cytochrome P450 enzymes involved in cuticular hydrocarbon synthesis. *Mol Phylogenet Evol,* 143**,** 106695.

FIELD, L. M. & DEVONSHIRE, A. L. 1998. Evidence that the E4 and FE4 esterase genes responsible for insecticide resistance in the aphid Myzus persicae (Sulzer) are part of a gene family. *Biochem J,* 330 (Pt 1)**,** 169-73.

FORNECK, A., WALKER, M. A. & BLAICH, R. 2001. Ecological and genetic aspects of grape phylloxera Daktulosphaira vitifoliae (Hemiptera: Phylloxeridae) performance on rootstock hosts. *Bull Entomol Res,* 91**,** 445-51.

GAWANDE, N. D., SUBASHINI, S., MURUGAN, M. & SUBBARAYALU, M. 2014. Molecular screening of insecticides with sigma glutathione S-transferases (GST) in cotton aphid Aphis gossypii using docking. *Bioinformation,* 10**,** 679-683.

GIARDINE, B., RIEMER, C., HARDISON, R. C., BURHANS, R., ELNITSKI, L., SHAH, P., ZHANG, Y., BLANKENBERG, D., ALBERT, I., TAYLOR, J., MILLER, W., KENT, W. J. & NEKRUTENKO, A. 2005. Galaxy: a platform for interactive large-scale genome analysis. *Genome Res,* 15**,** 1451-5.

GRBIC, M., VAN LEEUWEN, T., CLARK, R. M., ROMBAUTS, S., ROUZE, P., GRBIC, V., OSBORNE, E. J., DERMAUW, W., NGOC, P. C., ORTEGO, F., HERNANDEZ-CRESPO, P., DIAZ, I., MARTINEZ, M., NAVAJAS, M., SUCENA, E., MAGALHAES, S., NAGY, L., PACE, R. M., DJURANOVIC, S., SMAGGHE, G., IGA, M., CHRISTIAENS, O., VEENSTRA, J. A., EWER, J., VILLALOBOS, R. M., HUTTER, J. L., HUDSON, S. D., VELEZ, M., YI, S. V., ZENG, J., PIRES-DASILVA, A., ROCH, F., CAZAUX, M., NAVARRO, M., ZHUROV, V., ACEVEDO, G., BJELICA, A., FAWCETT, J. A., BONNET, E., MARTENS, C., BAELE, G., WISSLER, L., SANCHEZ-RODRIGUEZ, A., TIRRY, L., BLAIS, C., DEMEESTERE, K., HENZ, S. R., GREGORY, T. R., MATHIEU, J., VERDON, L., FARINELLI, L., SCHMUTZ, J., LINDQUIST, E., FEYEREISEN, R. & VAN DE PEER, Y. 2011. The genome of Tetranychus urticae reveals herbivorous pest adaptations. *Nature,* 479**,** 487-492.

GROEN, S. C., LAPLANTE, E. R., ALEXANDRE, N. M., AGRAWAL, A. A., DOBLER, S. & WHITEMAN, N. K. 2017. Multidrug transporters and organic anion transporting polypeptides protect insects against the toxic effects of cardenolides. *Insect Biochem Mol Biol,* 81**,** 51-61.

GUINDON, S., DUFAYARD, J.-F., LEFORT, V., ANISIMOVA, M., HORDIJK, W. & GASCUEL, O. 2010. New Algorithms and Methods to Estimate Maximum-Likelihood Phylogenies: Assessing the Performance of PhyML 3.0. *Systematic Biology,* 59**,** 307-321.

GUO, L., XIE, W., YANG, Z., XU, J. & ZHANG, Y. 2020. Genome-Wide Identification and Expression Analysis of Udp-Glucuronosyltransferases in the Whitefly Bemisia Tabaci (Gennadius) (HemipterA: Aleyrodidae). *International Journal of Molecular Sciences,* 21.

HEIDEL-FISCHER, H. M. & VOGEL, H. 2015. Molecular mechanisms of insect adaptation to plant secondary compounds. *Curr Opin Insect Sci,* 8**,** 8-14.

HELVIG, C., KOENER, J. F., UNNITHAN, G. C. & FEYEREISEN, R. 2004. CYP15A1, the cytochrome P450 that catalyzes epoxidation of methyl farnesoate to juvenile hormone III in cockroach corpora allata. *Proc Natl Acad Sci U S A,* 101**,** 4024-9.

HOCK, T., COTTRILL, T., KEEGAN, J. & GARZA, D. 2000. The *E23* early gene of Drosophila encodes an ecdysone-inducible ATP-binding cassette transporter capable of repressing ecdysone-mediated gene activation. *Proceedings of the National Academy of Sciences,* 97**,** 9519-9524.

HOPKINS, T. L. & KRAMER, K. J. 1992. Insect Cuticle Sclerotization. *Annual Review of Entomology,* 37**,** 273-302.

HUANG, F.-F., CHAI, C.-L., ZHANG, Z., LIU, Z.-H., DAI, F.-Y., LU, C. & XIANG, Z.-H. 2008. The UDP-glucosyltransferase multigene family in Bombyx mori. *BMC Genomics,* 9**,** 563.

INTERNATIONAL APHID GENOMICS, C. 2010. Genome sequence of the pea aphid Acyrthosiphon pisum. *PLoS Biol,* 8**,** e1000313.

ISHIKAWA, A., OGAWA K FAU - GOTOH, H., GOTOH H FAU - WALSH, T. K., WALSH TK FAU - TAGU, D., TAGU D FAU - BRISSON, J. A., BRISSON JA FAU - RISPE, C., RISPE C FAU - JAUBERT-POSSAMAI, S., JAUBERT-POSSAMAI S FAU - KANBE, T., KANBE T FAU - TSUBOTA, T., TSUBOTA T FAU - SHIOTSUKI, T., SHIOTSUKI T FAU - MIURA, T. & MIURA, T. 2012. Juvenile hormone titre and related gene expression during the change of reproductive modes in the pea aphid. *Insect Mol Biol,* 21**,** 49-60.

JAKOBY, W. B., . & ZIEGLER, D. M. 1990. The enzymes of detoxication. *J Biol Chem.,* 265**,** 20715-8.

JI, R., LEI, J., CHEN, I. W., SANG, W., YANG, S., FANG, J. & ZHU-SALZMAN, K. 2020. Cytochrome P450s CYP380C6 and CYP380C9 in green peach aphid facilitate its adaptation to indole glucosinolate-mediated plant defense. *Pest Manag Sci*.

KALOGERAKI, V. S., ZHU, J., EBERHARD, A., MADSEN, E. L. & WINANS, S. C. 1999. The phenolic vir gene inducer ferulic acid is O-demethylated by the VirH2 protein of an Agrobacterium tumefaciens Ti plasmid. *Mol Microbiol,* 34**,** 512-22.

KATOH, K., ROZEWICKI, J. & YAMADA, K. D. 2019. MAFFT online service: multiple sequence alignment, interactive sequence choice and visualization. *Brief Bioinform,* 20**,** 1160-1166.

KELLOW, A. V., SEDGLEY, M. & VAN HEESWIJCK, R. 2004. Interaction between Vitis vinifera and grape phylloxera: changes in root tissue during nodosity formation. *Ann Bot,* 93**,** 581-90.

KOVALCHUK, A. & DRIESSEN, A. J. 2010. Phylogenetic analysis of fungal ABC transporters. *BMC Genomics,* 11**,** 177.

KOWALSKI, P., BAUM, M., KORTEN, M., DONATH, A. & DOBLER, S. 2020. ABCB transporters in a leaf beetle respond to sequestered plant toxins. *Proc Biol Sci,* 287**,** 20201311.

KUMAR, S., STECHER, G., SULESKI, M. & HEDGES, S. B. 2017. TimeTree: A Resource for Timelines, Timetrees, and Divergence Times. *Mol Biol Evol,* 34**,** 1812-1819.

LAWO, N. C., WEINGART, G. J., SCHUHMACHER, R. & FORNECK, A. 2011. The volatile metabolome of grapevine roots: first insights into the metabolic response upon phylloxera attack. *Plant Physiol Biochem,* 49**,** 1059-63.

LEFORT, V., LONGUEVILLE, J.-E. & GASCUEL, O. 2017. SMS: Smart Model Selection in PhyML. *Molecular Biology and Evolution,* 34**,** 2422-2424.

LOUGHRIN, J. H., POTTER, D. A., HAMILTON-KEMP, T. R. & BYERS, M. E. 1997. Diurnal emission of volatile compounds by Japanese beetle-damaged grape leaves. *Phytochemistry,* 45**,** 919-923.

MATHERS, T. C., CHEN, Y., KAITHAKOTTIL, G., LEGEAI, F., MUGFORD, S. T., BAA-PUYOULET, P., BRETAUDEAU, A., CLAVIJO, B., COLELLA, S., COLLIN, O., DALMAY, T., DERRIEN, T., FENG, H., GABALDON, T., JORDAN, A., JULCA, I., KETTLES, G. J., KOWITWANICH, K., LAVENIER, D., LENZI, P., LOPEZ-GOMOLLON, S., LOSKA, D., MAPLESON, D., MAUMUS, F., MOXON, S., PRICE, D. R., SUGIO, A., VAN MUNSTER, M., UZEST, M., WAITE, D., JANDER, G., TAGU, D., WILSON, A. C., VAN OOSTERHOUT, C., SWARBRECK, D. & HOGENHOUT, S. A. 2017. Rapid transcriptional plasticity of duplicated gene clusters enables a clonally reproducing aphid to colonise diverse plant species. *Genome Biol,* 18**,** 27.

MORGAN, T. H. 1910. Sex limited inheritance in drosophila. *Science,* 32**,** 120-122.

MORITA, M. & IMANAKA, T. 2012. Peroxisomal ABC transporters: structure, function and role in disease. *Biochim Biophys Acta,* 1822**,** 1387-96.

MURRAY, C. L., QUAGLIA M FAU - ARNASON, J. T., ARNASON JT FAU - MORRIS, C. E. & MORRIS, C. E. 1994. A putative nicotine pump at the metabolic blood-brain barrier of the tobacco hornworm. *J Neurobiol.,* 25**,** 23-34.

NABESHIMA, T., KOZAKI, T., TOMITA, T. & KONO, Y. 2003. An amino acid substitution on the second acetylcholinesterase in the pirimicarb-resistant strains of the peach potato aphid, Myzus persicae. *Biochem Biophys Res Commun,* 307**,** 15-22.

NABITY, P. D., HAUS, M. J., BERENBAUM, M. R. & DELUCIA, E. H. 2013. Leaf-galling phylloxera on grapes reprograms host metabolism and morphology. *Proc Natl Acad Sci U S A,* 110**,** 16663-8.

NICHOLSON, S. J., NICKERSON, M. L., DEAN, M., SONG, Y., HOYT, P. R., RHEE, H., KIM, C. & PUTERKA, G. J. 2015. The genome of Diuraphis noxia, a global aphid pest of small grains. *BMC Genomics,* 16**,** 429.

OAKESHOTT, J. G., DEVONSHIRE, A. L., CLAUDIANOS, C., SUTHERLAND, T. D., HORNE, I., CAMPBELL, P. M., OLLIS, D. L. & RUSSELL, R. J. 2005. Comparing the organophosphorus and carbamate insecticide resistance mutations in cholin- and carboxyl-esterases. *Chem Biol Interact,* 157-158**,** 269-75.

OAKESHOTT, J. G., JOHNSON, R. M., BERENBAUM, M. R., RANSON, H., CRISTINO, A. S. & CLAUDIANOS, C. 2010. Metabolic enzymes associated with xenobiotic and chemosensory responses in Nasonia vitripennis. *Insect Mol Biol,* 19 Suppl 1**,** 147-63.

PAN, Y., TIAN, F., WEI, X., WU, Y., GAO, X., XI, J. & SHANG, Q. 2018. Thiamethoxam Resistance in Aphis gossypii Glover Relies on Multiple UDP-Glucuronosyltransferases. *Frontiers in Physiology,* 9.

PAN, Y., XU, P., ZENG, X., LIU, X. & SHANG, Q. 2019. Characterization of UDP-Glucuronosyltransferases and the Potential Contribution to Nicotine Tolerance in Myzus persicae. *International Journal of Molecular Sciences,* 20**,** 3637.

PEDRA, J. H. F., MCINTYRE, L. M., SCHARF, M. E. & PITTENDRIGH, B. R. 2004. Genome-wide transcription profile of field- and laboratory-selected dichlorodiphenyltrichloroethane (DDT)-resistant *Drosophila*. *Proceedings of the National Academy of Sciences of the United States of America,* 101**,** 7034.

PETRYK, A., WARREN, J. T., MARQUES, G., JARCHO, M. P., GILBERT, L. I., KAHLER, J., PARVY, J. P., LI, Y., DAUPHIN-VILLEMANT, C. & O'CONNOR, M. B. 2003. Shade is the Drosophila P450 enzyme that mediates the hydroxylation of ecdysone to the steroid insect molting hormone 20-hydroxyecdysone. *Proc Natl Acad Sci U S A,* 100**,** 13773-8.

PETSCHENKA, G., PICK, C., WAGSCHAL, V. & DOBLER, S. 2013. Functional evidence for physiological mechanisms to circumvent neurotoxicity of cardenolides in an adapted and a non-adapted hawk-moth species. *Proc Biol Sci,* 280**,** 20123089.

POPOVIC, M., ZAJA, R., LONCAR, J. & SMITAL, T. 2010. A novel ABC transporter: the first insight into zebrafish (Danio rerio) ABCH1. *Mar Environ Res,* 69**,** Suppl: S11-13.

POWELL, K. S., COOPER, P. D. & FORNECK, A. 2013. The Biology, Physiology and Host–Plant Interactions of Grape Phylloxera Daktulosphaira vitifoliae. *Behaviour and Physiology of Root Herbivores.*

PYM, A., SINGH, K. S., NORDGREN, A., DAVIES, T. G. E., ZIMMER, C. T., ELIAS, J., SLATER, R. & BASS, C. 2019. Host plant adaptation in the polyphagous whitefly, Trialeurodes vaporariorum, is associated with transcriptional plasticity and altered sensitivity to insecticides. *BMC Genomics,* 20**,** 996.

QI, W., MA, X., HE, W., CHEN, W., ZOU, M., GURR, G. M., VASSEUR, L. & YOU, M. 2016. Characterization and expression profiling of ATP-binding cassette transporter genes in the diamondback moth, Plutella xylostella (L.). *BMC Genomics,* 17**,** 760.

QIU, Y., TITTIGER, C., WICKER-THOMAS, C., LE GOFF, G., YOUNG, S., WAJNBERG, E., FRICAUX, T., TAQUET, N., BLOMQUIST, G. J. & FEYEREISEN, R. 2012. An insect-specific P450 oxidative decarbonylase for cuticular hydrocarbon biosynthesis. *Proc Natl Acad Sci U S A,* 109**,** 14858-63.

RAMSEY, J. S., RIDER, D. S., WALSH, T. K., DE VOS, M., GORDON, K. H., PONNALA, L., MACMIL, S. L., ROE, B. A. & JANDER, G. 2010. Comparative analysis of detoxification enzymes in Acyrthosiphon pisum and Myzus persicae. *Insect Mol Biol,* 19 Suppl 2**,** 155-64.

RASMANN, S., KOLLNER, T. G., DEGENHARDT, J., HILTPOLD, I., TOEPFER, S., KUHLMANN, U., GERSHENZON, J. & TURLINGS, T. C. 2005. Recruitment of entomopathogenic nematodes by insect-damaged maize roots. *Nature,* 434**,** 732-7.

RICHMOND, R. C., GILBERT, D. G., SHEEHAN, K. B., GROMKO, M. H. & BUTTERWORTH, F. M. 1980. Esterase 6 and reproduction in Drosophila melanogaster. *Science,* 207**,** 1483.

RISPE, C., LEGEAI, F., NABITY, P. D., FERNANDEZ, R., ARORA, A. K., BAA-PUYOULET, P., BANFILL, C. R., BAO, L., BARBERA, M., BOUALLEGUE, M., BRETAUDEAU, A., BRISSON, J. A., CALEVRO, F., CAPY, P., CATRICE, O., CHERTEMPS, T., COUTURE, C., DELIERE, L., DOUGLAS, A. E., DUFAULT-THOMPSON, K., ESCUER, P., FENG, H., FORNECK, A., GABALDON, T., GUIGO, R., HILLIOU, F., HINOJOSA-ALVAREZ, S., HSIAO, Y. M., HUDAVERDIAN, S., JACQUIN-JOLY, E., JAMES, E. B., JOHNSTON, S., JOUBARD, B., LE GOFF, G., LE TRIONNAIRE, G., LIBRADO, P., LIU, S., LOMBAERT, E., LU, H. L., MAIBECHE, M., MAKNI, M., MARCET-HOUBEN, M., MARTINEZ-TORRES, D., MESLIN, C., MONTAGNE, N., MORAN, N. A., PAPURA, D., PARISOT, N., RAHBE, Y., LOPES, M. R., RIPOLL-CLADELLAS, A., ROBIN, S., ROQUES, C., ROUX, P., ROZAS, J., SANCHEZ-GRACIA, A., SANCHEZ-HERRERO, J. F., SANTESMASSES, D., SCATONI, I., SERRE, R. F., TANG, M., TIAN, W., UMINA, P. A., VAN MUNSTER, M., VINCENT-MONEGAT, C., WEMMER, J., WILSON, A. C. C., ZHANG, Y., ZHAO, C., ZHAO, J., ZHAO, S., ZHOU, X., DELMOTTE, F. & TAGU, D. 2020. The genome sequence of the grape phylloxera provides insights into the evolution, adaptation, and invasion routes of an iconic pest. *BMC Biol,* 18**,** 90.

RISPE, C., LEGEAI, F., PAPURA, D., BRETAUDEAU, A., HUDAVERDIAN, S., LE TRIONNAIRE, G., TAGU, D., JAQUIERY, J. & DELMOTTE, F. 2016. De novo transcriptome assembly of the grapevine phylloxera allows identification of genes differentially expressed between leaf- and root-feeding forms. *BMC Genomics,* 17**,** 219.

SAVOI, S., EITLE, M. W., BERGER, H., CURTO, M., MEIMBERG, H., GRIESSER, M. & FORNECK, A. 2020. Comparative Transcriptome Analysis of Two Root-Feeding Grape Phylloxera (D. vitifoliae) Lineages Feeding on a Rootstock and V. vinifera. *Insects,* 11.

SCHAEDLER, T. A., FAUST, B., SHINTRE, C. A., CARPENTER, E. P., SRINIVASAN, V., VAN VEEN, H. W. & BALK, J. 2015. Structures and functions of mitochondrial ABC transporters. *Biochem Soc Trans,* 43**,** 943-51.

SCHAMA, R., PEDRINI, N., JUAREZ, M. P., NELSON, D. R., TORRES, A. Q., VALLE, D. & MESQUITA, R. D. 2016. Rhodnius prolixus supergene families of enzymes potentially associated with insecticide resistance. *Insect Biochem Mol Biol,* 69**,** 91-104.

SCHULTZ, J. C., EDGER, P. P., BODY, M. J. A. & APPEL, H. M. 2019. A galling insect activates plant reproductive programs during gall development. *Sci Rep,* 9**,** 1833.

SCHUMANN, I., KENNY, N., HUI, J., HERING, L. & MAYER, G. 2018a. Halloween genes in panarthropods and the evolution of the early moulting pathway in Ecdysozoa. *Royal Society Open Science,* 5**,** 180888.

SCHUMANN, I., KENNY, N., HUI, J., HERING, L. & MAYER, G. 2018b. Halloween genes in panarthropods and the evolution of the early moulting pathway in Ecdysozoa. *R Soc Open Sci,* 5**,** 180888.

SCOTT, D. 1986. INHIBITION OF FEMALE DROSOPHILA MELANOGASTER REMATING BY A SEMINAL FLUID PROTEIN (ESTERASE 6). *Evolution,* 40**,** 1084-1091.

SHEEHAN, D., MEADE, G., FOLEY, V. M. & DOWD, C. A. 2001. Structure, function and evolution of glutathione transferases: implications for classification of non-mammalian members of an ancient enzyme superfamily. *The Biochemical journal,* 360**,** 1-16.

SILVA, A. X., JANDER, G., SAMANIEGO, H., RAMSEY, J. S. & FIGUEROA, C. C. 2012. Insecticide Resistance Mechanisms in the Green Peach Aphid Myzus persicae (Hemiptera: Aphididae) I: A Transcriptomic Survey. *PLOS ONE,* 7**,** e36366.

STURM, A., CUNNINGHAM, P. & DEAN, M. 2009. The ABC transporter gene family of Daphnia pulex. *BMC Genomics,* 10**,** 170.

SUN, H., BUCHON, N. & SCOTT, J. G. 2017a. Mdr65 decreases toxicity of multiple insecticides in Drosophila melanogaster. *Insect Biochem Mol Biol,* 89**,** 11-16.

SUN, H., PU, J., CHEN, F., WANG, J. & HAN, Z. 2017b. Multiple ATP-binding cassette transporters are involved in insecticide resistance in the small brown planthopper, Laodelphax striatellus. *Insect Mol Biol.,* 26**,** 343-355.

TATEMATSU, K.-I., YAMAMOTO, K., UCHINO, K., NARUKAWA, J., IIZUKA, T., BANNO, Y., KATSUMA, S., SHIMADA, T., TAMURA, T., SEZUTSU, H. & DAIMON, T. 2011. Positional cloning of silkworm white egg 2 (w-2) locus shows functional conservation and diversification of ABC transporters for pigmentation in insects. *Genes to Cells,* 16**,** 331-342.

TAY, W. T., MAHON, R. J., HECKEL, D. G., WALSH, T. K., DOWNES, S., JAMES, W. J., LEE, S.-F., REINEKE, A., WILLIAMS, A. K. & GORDON, K. H. J. 2015. Insect Resistance to Bacillus thuringiensis Toxin Cry2Ab Is Conferred by Mutations in an ABC Transporter Subfamily A Protein. *PLOS Genetics,* 11**,** e1005534.

TIAN, F., WANG, Z., LI, C., LIU, J. & ZENG, X. 2019. UDP-Glycosyltransferases are involved in imidacloprid resistance in the Asian citrus psyllid, Diaphorina citri (Hemiptera: Lividae). *Pesticide Biochemistry and Physiology,* 154**,** 23-31.

TIAN, L., SONG, T., HE, R., ZENG, Y., XIE, W., WU, Q., WANG, S., ZHOU, X. & ZHANG, Y. 2017. Genome-wide analysis of ATP-binding cassette (ABC) transporters in the sweetpotato whitefly, Bemisia tabaci. *BMC Genomics,* 18**,** 330.

TOBA, G. & AIGAKI, T. 2000. Disruption of the Microsomal glutathione S-transferase-like gene reduces life span of Drosophila melanogaster. *Gene,* 253**,** 179-187.

TRAVERSO, L., LAVORE, A., SIERRA, I., PALACIO, V., MARTINEZ-BARNETCHE, J., LATORRE-ESTIVALIS, J. M., MOUGABURE-CUETO, G., FRANCINI, F., LORENZO, M. G., RODRÍGUEZ, M. H., ONS, S. & RIVERA-POMAR, R. V. 2017. Comparative and functional triatomine genomics reveals reductions and expansions in insecticide resistance-related gene families. *PLoS neglected tropical diseases,* 11**,** e0005313-e0005313.

TUCKER, D. J., LAMB, D. L., POWELL, K. S., BLANCHFIELD, A. L. & BRERETON, I. M. 2007. Detection of phylloxera infestation in grapevines by NMR methods.

VERRIER, P. J., BIRD, D., BURLA, B., DASSA, E., FORESTIER, C., GEISLER, M., KLEIN, M., KOLUKISAOGLU, U., LEE, Y., MARTINOIA, E., MURPHY, A., REA, P. A., SAMUELS, L., SCHULZ, B., SPALDING, E. J., YAZAKI, K. & THEODOULOU, F. L. 2008. Plant ABC proteins--a unified nomenclature and updated inventory. *Trends Plant Sci,* 13**,** 151-9.

VONTAS, J., BLASS, C., KOUTSOS, A. C., DAVID, J. P., KAFATOS, F. C., LOUIS, C., HEMINGWAY, J., CHRISTOPHIDES, G. K. & RANSON, H. 2005. Gene expression in insecticide resistant and susceptible Anopheles gambiae strains constitutively or after insecticide exposure. *Insect Molecular Biology,* 14**,** 509-521.

VONTAS, J. G., SMALL, G. J., NIKOU, D. C., RANSON, H. & HEMINGWAY, J. 2002. Purification, molecular cloning and heterologous expression of a glutathione S-transferase involved in insecticide resistance from the rice brown planthopper, Nilaparvata lugens. *The Biochemical journal,* 362**,** 329-337.

WANG, Y., NORUM, M., OEHL, K., YANG, Y., ZUBER, R., YANG, J., FARINE, J. P., GEHRING, N., FLOTENMEYER, M., FERVEUR, J. F. & MOUSSIAN, B. 2020. Dysfunction of Oskyddad causes Harlequin-type ichthyosis-like defects in Drosophila melanogaster. *PLoS Genet,* 16**,** e1008363.

WENZEL, J. J., PIEHLER, A. & KAMINSKI, W. E. 2007. ABC A-subclass proteins: gatekeepers of cellular phospho- and sphingolipid transport. *Front Biosci,* 12**,** 3177-93.

WILLINGHAM, A. T. & KEIL, T. 2004. A tissue specific cytochrome P450 required for the structure and function of Drosophila sensory organs. *Mech Dev,* 121**,** 1289-97.

WU, L., JIA, Q., ZHANG, X., ZHANG, X., LIU, S., PARK, Y., FEYEREISEN, R., ZHU, K. Y., MA, E., ZHANG, J. & LI, S. 2019. CYP303A1 has a conserved function in adult eclosion in Locusta migratoria and Drosophila melanogaster. *Insect Biochem Mol Biol,* 113**,** 103210.

WU, L., YU, Z., JIA, Q., ZHANG, X., MA, E., LI, S., ZHU, K. Y., FEYEREISEN, R. & ZHANG, J. 2020. Knockdown of LmCYP303A1 alters cuticular hydrocarbon profiles and increases the susceptibility to desiccation and insecticides in Locusta migratoria. *Pestic Biochem Physiol,* 168**,** 104637.

XIA, J., XU, H., YANG, Z., PAN, H., YANG, X., GUO, Z., YANG, F., GUO, L., SUN, X., WANG, S., WU, Q., XIE, W. & ZHANG, Y. 2019. Genome-Wide Analysis of Carboxylesterases (COEs) in the Whitefly, Bemisia tabaci (Gennadius). *Int J Mol Sci,* 20.

YAMAMOTO, K., SHIGEOKA, Y., ASO, Y., BANNO, Y., KIMURA, M. & NAKASHIMA, T. 2009. Molecular and biochemical characterization of a Zeta-class glutathione S-transferase of the silkmoth. *Pesticide Biochemistry and Physiology,* 94**,** 30-35.

YAMAMOTO, K. & YAMADA, N. 2016. Identification of a diazinon-metabolizing glutathione S-transferase in the silkworm, Bombyx mori. *Scientific Reports,* 6**,** 30073.

YANG, N., XIE, W., YANG, X., WANG, S., WU, Q., LI, R., PAN, H., LIU, B., SHI, X., FANG, Y., XU, B., ZHOU, X. & ZHANG, Y. 2013. Transcriptomic and Proteomic Responses of Sweetpotato Whitefly, Bemisia tabaci, to Thiamethoxam. *PLOS ONE,* 8**,** e61820.

YU, Q. Y., LU, C., LI, W. L., XIANG, Z. H. & ZHANG, Z. 2009. Annotation and expression of carboxylesterases in the silkworm, Bombyx mori. *BMC Genomics,* 10**,** 553.

YU, Z., WANG, Y., ZHAO, X., LIU, X., MA, E., MOUSSIAN, B. & ZHANG, J. 2017. The ABC transporter ABCH-9C is needed for cuticle barrier construction in Locusta migratoria. *Insect biochemistry and molecular biology,* 87**,** 90-99.

ZHANG, H., GUIGUET, A., DUBREUIL, G., KISIALA, A., ANDREAS, P., EMERY, R. J. N., HUGUET, E., BODY, M. & GIRON, D. 2017. Dynamics and origin of cytokinins involved in plant manipulation by a leaf-mining insect. *Insect Sci,* 24**,** 1065-1078.

ZHANG, N.-N., LIU, C.-F., YANG, F., DONG, S.-L. & HAN, Z.-J. 2012. Resistance mechanisms to chlorpyrifos and F392W mutation frequencies in the acetylcholine esterase ace1 allele of field populations of the tobacco whitefly, Bemisia tabaci in China. *Journal of insect science (Online),* 12**,** 41-41.

ZHANG, S. D. & ODENWALD, W. F. 1995. Misexpression of the white (w) gene triggers male-male courtship in Drosophila. *Proceedings of the National Academy of Sciences of the United States of America,* 92**,** 5525-5529.

ZHAO, J.-J., FAN, D.-S., ZHANG, Y. & FENG, J.-N. 2017. Identification and Characterisation of Putative Glutathione S-Transferase Genes from Daktulosphaira vitifoliae (Hemiptera: Phylloxeridae). *Environmental Entomology,* 47**,** 196-203.

ZHOU, W.-W., LIANG, Q.-M., XU, Y., GURR, G. M., BAO, Y.-Y., ZHOU, X.-P., ZHANG, C.-X., CHENG, J. & ZHU, Z.-R. 2013. Genomic insights into the glutathione S-transferase gene family of two rice planthoppers, Nilaparvata lugens (Stål) and Sogatella furcifera (Horváth) (Hemiptera: Delphacidae). *PloS one,* 8**,** e56604-e56604.

ZUBER, R., NORUM, M., WANG, Y., OEHL, K., GEHRING, N., ACCARDI, D., BARTOZSEWSKI, S., BERGER, J., FLOTENMEYER, M. & MOUSSIAN, B. 2018. The ABC transporter Snu and the extracellular protein Snsl cooperate in the formation of the lipid-based inward and outward barrier in the skin of Drosophila. *Eur J Cell Biol,* 97**,** 90-101.

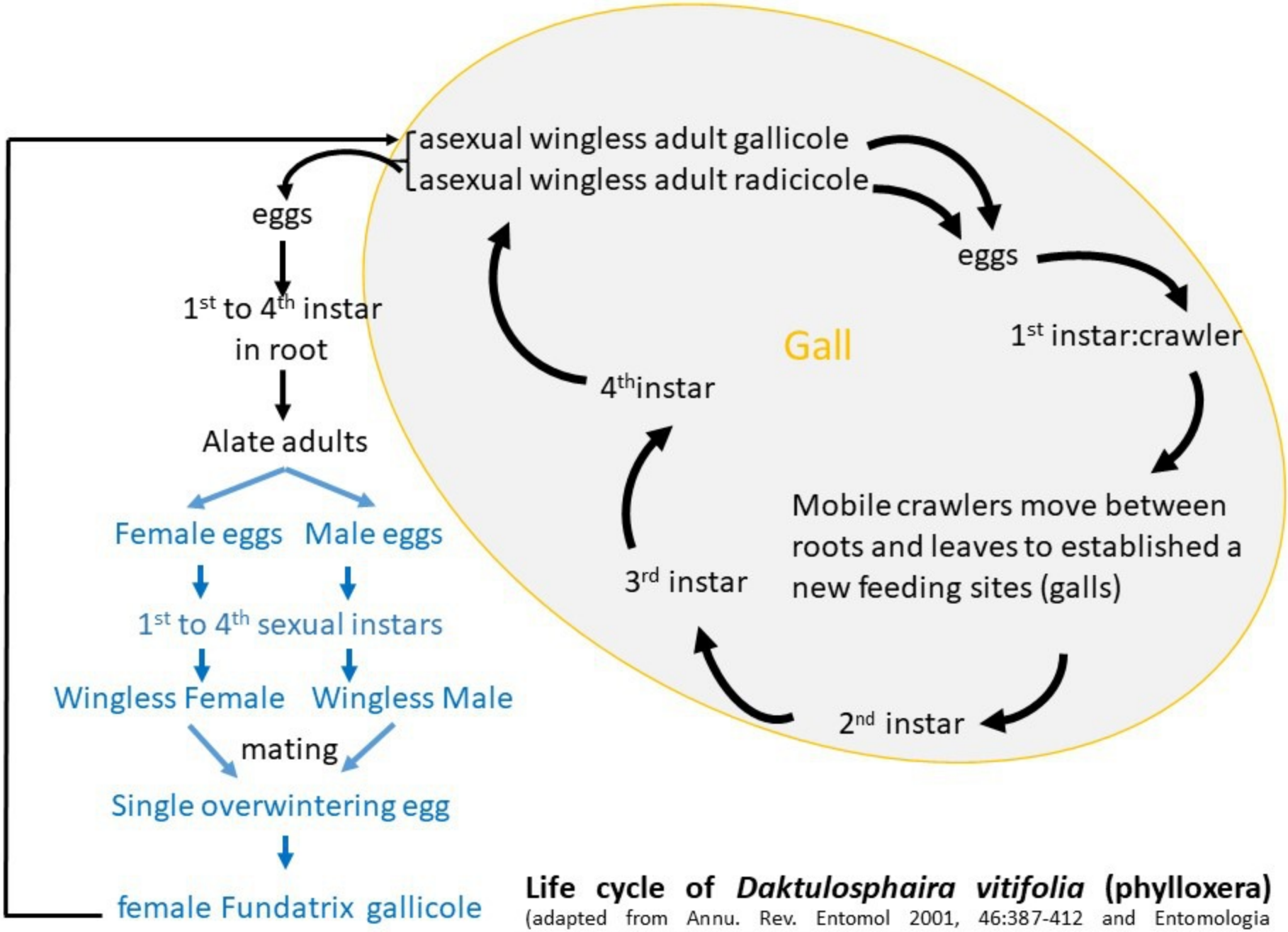

Life cycle of *Daktulosphaira vitifolia* (phylloxera)
(adapted from Annu. Rev. Entomol 2001, 46:387-412 and Entomologia experimentalis et applicata. 2009 vol: 131 (1) pp: :1-10)

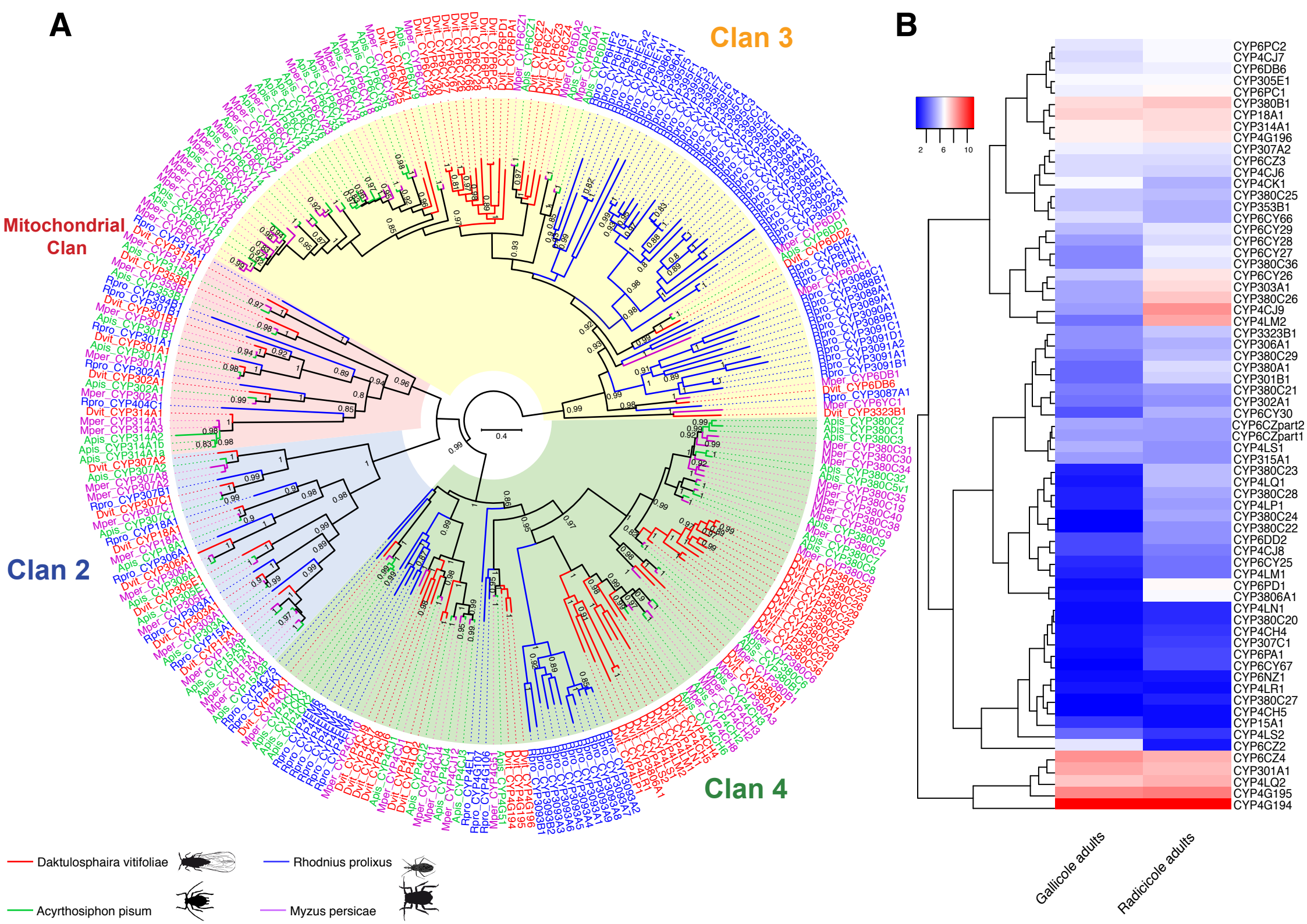
A
Clan 3
Mitochondrial Clan
Clan 2
Clan 4
0.4
B
CYP6PC2
CYP4CJ7
CYP6DB6
CYP305E1
CYP6PC1
CYP380B1
CYP18A1
CYP314A1
CYP4G196
CYP307A2
CYP6CZ3
CYP4CJ6
CYP4CK1
CYP380C25
CYP353B1
CYP6CY66
CYP6CY29
CYP6CY28
CYP6CY27
CYP380C36
CYP6CY26
CYP303A1
CYP380C26
CYP4CJ9
CYP4LM2
CYP3323B1
CYP306A1
CYP380C29
CYP380A1
CYP301B1
CYP380C21
CYP302A1
CYP6CY30
CYP6CZpart2
CYP6CZpart1
CYP4LS1
CYP315A1
CYP380C23
CYP4LQ1
CYP380C28
CYP4LP1
CYP380C24
CYP380C22
CYP6DD2
CYP4CJ8
CYP6CY25
CYP4LM1
CYP6PD1
CYP3806A1
CYP4LN1
CYP380C20
CYP4CH4
CYP307C1
CYP6PA1
CYP6CY67
CYP6NZ1
CYP4LR1
CYP380C27
CYP4CH5
CYP15A1
CYP4LS2
CYP6CZ2
CYP6CZ4
CYP301A1
CYP4LQ2
CYP4G195
CYP4G194
2
6
10
Gallicole adults
Radicicole adults
Daktulosphaira vitifoliae
Acyrthosiphon pisum
Rhodnius prolixus
Myzus persicae

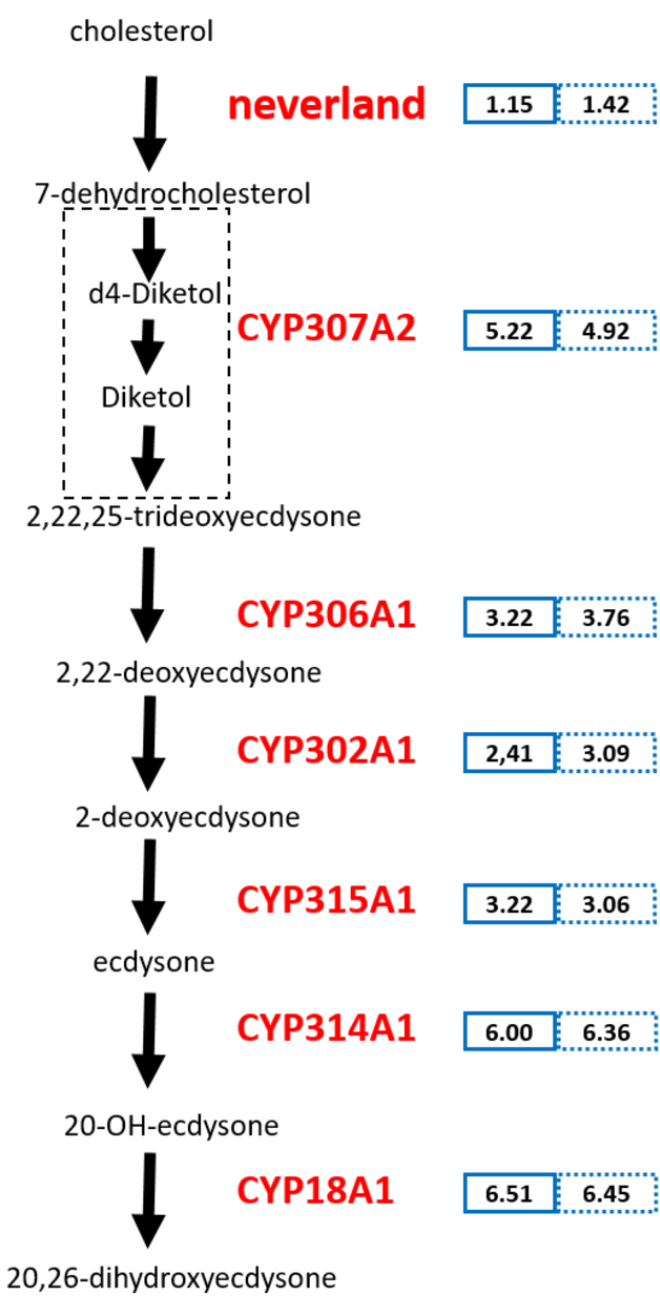
cholesterol
neverland
1.15
1.42
7-dehydrocholesterol
d4-Diketol
CYP307A2
5.22
4.92
Diketol
2,22,25-trideoxyecdysone
CYP306A1
3.22
3.76
2,22-deoxyecdysone
CYP302A1
2,41
3.09
2-deoxyecdysone
CYP315A1
3.22
3.06
ecdysone
CYP314A1
6.00
6.36
20-OH-ecdysone
CYP18A1
6.51
6.45
20,26-dihydroxyecdysone
GA
RA

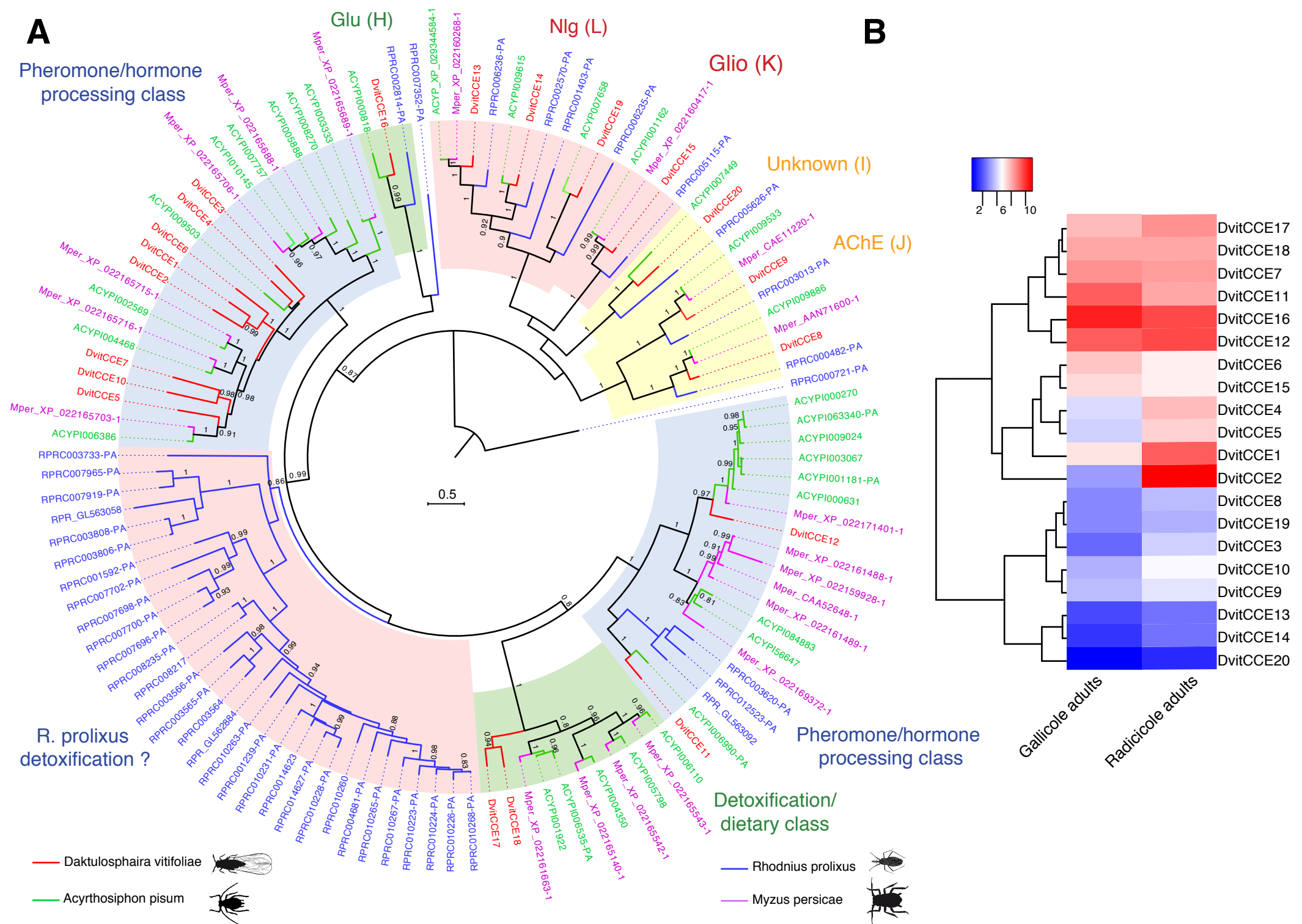
A
Glu (H)
Nlg (L)
Glio (K)
Unknown (I)
AChE (J)
Pheromone/hormone processing class
R. prolixus detoxification ?
Pheromone/hormone processing class
Detoxification/ dietary class
0.5
Daktulosphaira vitifoliae
Acyrthosiphon pisum
Rhodnius prolixus
Myzus persicae
B
2
6
10
DvitCCE17
DvitCCE18
DvitCCE7
DvitCCE11
DvitCCE16
DvitCCE12
DvitCCE6
DvitCCE15
DvitCCE4
DvitCCE5
DvitCCE1
DvitCCE2
DvitCCE8
DvitCCE19
DvitCCE3
DvitCCE10
DvitCCE9
DvitCCE13
DvitCCE14
DvitCCE20
Gallicole adults
Radicicole adults

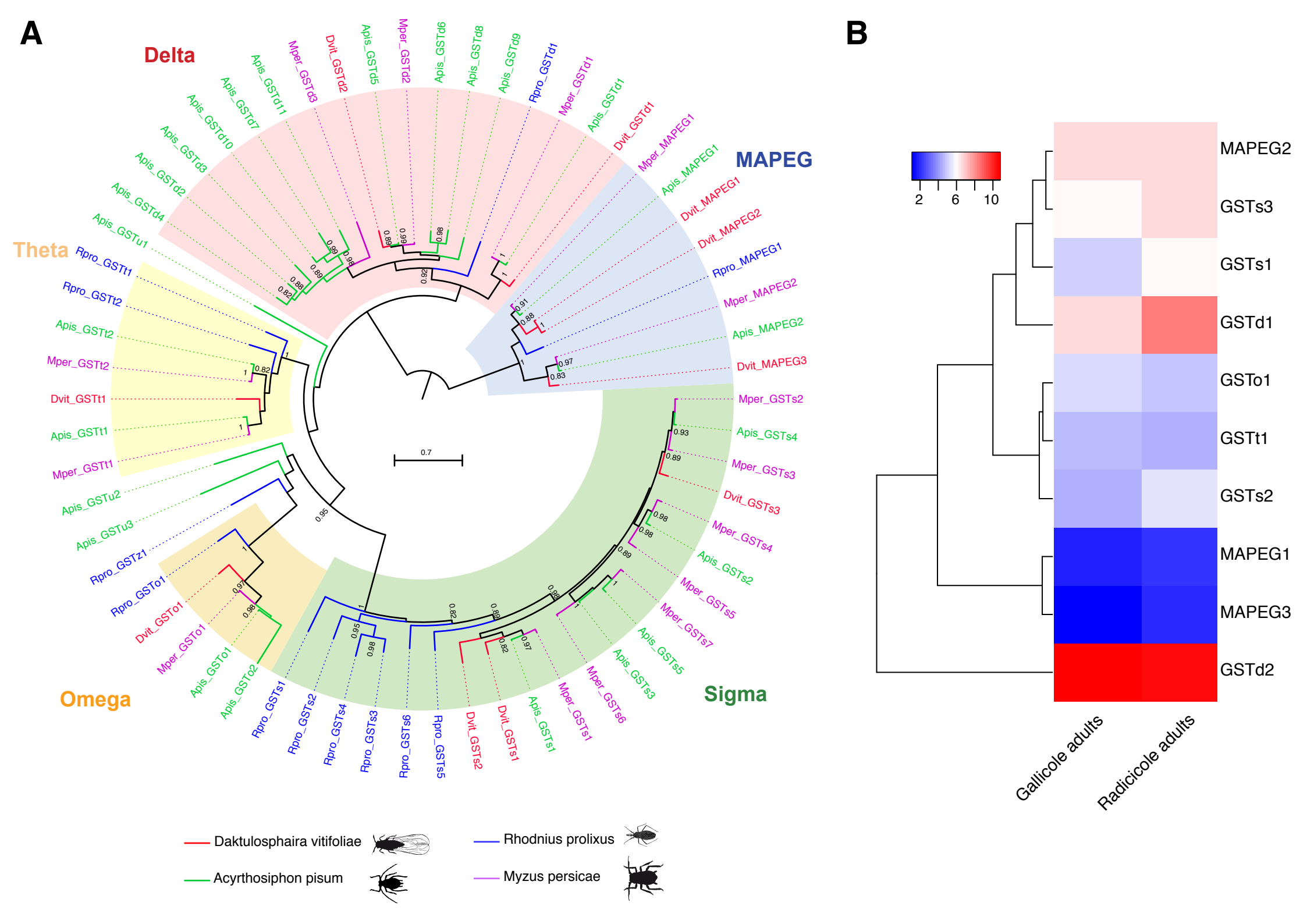
A
Delta
MAPEG
Theta
Omega
Sigma
Apis_GSTd1
Apis_GSTd2
Apis_GSTd3
Apis_GSTd4
Apis_GSTd5
Apis_GSTd6
Apis_GSTd7
Apis_GSTd8
Apis_GSTd9
Apis_GSTd10
Apis_GSTd11
Apis_GSTu1
Apis_GSTt1
Apis_GSTt2
Apis_GSTu2
Apis_GSTu3
Apis_GSTz1
Apis_GSTo1
Apis_GSTo2
Apis_MAPEG1
Apis_MAPEG2
Apis_GSTs1
Apis_GSTs2
Apis_GSTs3
Apis_GSTs4
Apis_GSTs5
Dvit_GSTd1
Dvit_GSTd2
Dvit_MAPEG1
Dvit_MAPEG2
Dvit_MAPEG3
Dvit_GSTt1
Dvit_GSTo1
Dvit_GSTs1
Dvit_GSTs2
Dvit_GSTs3
Mper_GSTd1
Mper_GSTd2
Mper_GSTd3
Mper_MAPEG1
Mper_MAPEG2
Mper_GSTt1
Mper_GSTt2
Mper_GSTo1
Mper_GSTs1
Mper_GSTs2
Mper_GSTs3
Mper_GSTs4
Mper_GSTs5
Mper_GSTs6
Mper_GSTs7
Rpro_GSTd1
Rpro_MAPEG1
Rpro_GSTt1
Rpro_GSTt2
Rpro_GSTz1
Rpro_GSTo1
Rpro_GSTs1
Rpro_GSTs2
Rpro_GSTs3
Rpro_GSTs4
Rpro_GSTs5
Rpro_GSTs6
0.7
Daktulosphaira vitifoliae
Acyrthosiphon pisum
Rhodnius prolixus
Myzus persicae
B
2
6
10
MAPEG2
GSTs3
GSTs1
GSTd1
GSTo1
GSTt1
GSTs2
MAPEG1
MAPEG3
GSTd2
Gallicole adults
Radicicole adults

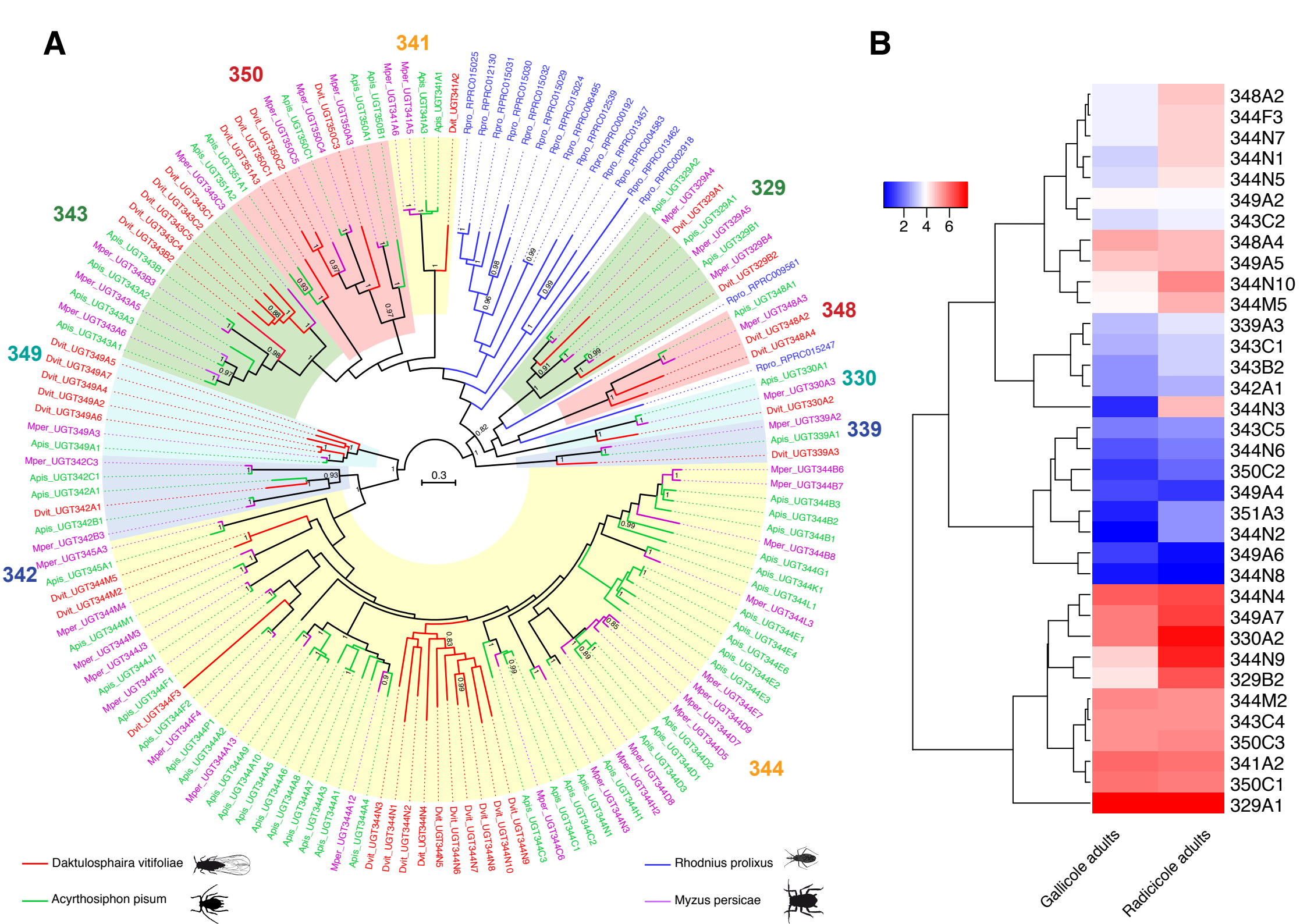
A
341
350
329
343
348
349
330
339
342
344
0.3
Daktulosphaira vitifoliae
Acyrthosiphon pisum
Rhodnius prolixus
Myzus persicae
B
2
4
6
348A2
344F3
344N7
344N1
344N5
349A2
343C2
348A4
349A5
344N10
344M5
339A3
343C1
343B2
342A1
344N3
343C5
344N6
350C2
349A4
351A3
344N2
349A6
344N8
344N4
349A7
330A2
344N9
329B2
344M2
343C4
350C3
341A2
350C1
329A1
Gallicole adults
Radicicole adults

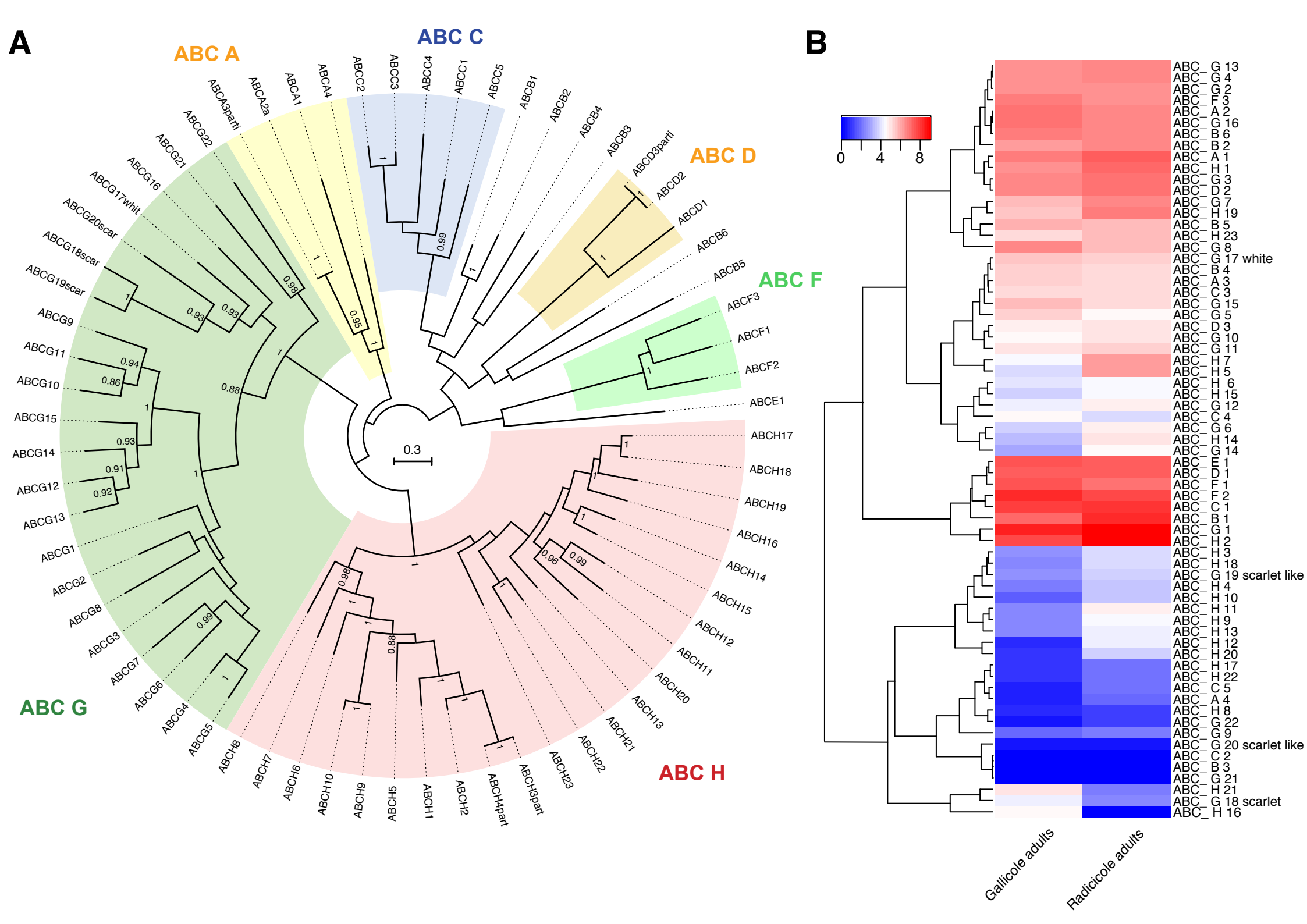
A
ABC A
ABC C
ABC D
ABC F
ABC G
ABC H
ABCA3parti
ABCA2a
ABCA1
ABCA4
ABCC2
ABCC3
ABCC4
ABCC1
ABCC5
ABCB1
ABCB2
ABCB4
ABCB3
ABCD3parti
ABCD2
ABCD1
ABCB6
ABCB5
ABCF3
ABCF1
ABCF2
ABCE1
ABCG22
ABCG21
ABCG16
ABCG17whit
ABCG20scar
ABCG18scar
ABCG19scar
ABCG9
ABCG11
ABCG10
ABCG15
ABCG14
ABCG12
ABCG13
ABCG1
ABCG2
ABCG8
ABCG3
ABCG7
ABCG6
ABCG4
ABCG5
ABCH8
ABCH7
ABCH6
ABCH10
ABCH9
ABCH5
ABCH1
ABCH2
ABCH4part
ABCH3part
ABCH23
ABCH22
ABCH21
ABCH13
ABCH20
ABCH11
ABCH12
ABCH15
ABCH14
ABCH16
ABCH19
ABCH18
ABCH17
0.3
B
0
4
8
ABC_ G 13
ABC_ G 4
ABC_ G 2
ABC_ F 3
ABC_ A 2
ABC_ G 16
ABC_ B 6
ABC_ B 2
ABC_ A 1
ABC_ H 1
ABC_ G 3
ABC_ D 2
ABC_ G 7
ABC_ H 19
ABC_ B 5
ABC_ H 23
ABC_ G 8
ABC_ G 17 white
ABC_ B 4
ABC_ A 3
ABC_ C 3
ABC_ G 15
ABC_ G 5
ABC_ D 3
ABC_ G 10
ABC_ G 11
ABC_ H 7
ABC_ H 5
ABC_ H 6
ABC_ H 15
ABC_ G 12
ABC_ C 4
ABC_ G 6
ABC_ H 14
ABC_ G 14
ABC_ E 1
ABC_ D 1
ABC_ F 1
ABC_ F 2
ABC_ C 1
ABC_ B 1
ABC_ G 1
ABC_ H 2
ABC_ H 3
ABC_ H 18
ABC_ G 19 scarlet like
ABC_ H 4
ABC_ H 10
ABC_ H 11
ABC_ H 9
ABC_ H 13
ABC_ H 12
ABC_ H 20
ABC_ H 17
ABC_ H 22
ABC_ C 5
ABC_ A 4
ABC_ H 8
ABC_ G 22
ABC_ G 9
ABC_ G 20 scarlet like
ABC_ C 2
ABC_ B 3
ABC_ G 21
ABC_ H 21
ABC_ G 18 scarlet
ABC_ H 16
Gallicole adults
Radicicole adults

Order	Hemiptera					
Species	*Daktulosphaira vitifoliae*	*Acyrthosiphon pisum*	*Rhodnius prolixus*	*Bemisia tabaci*	*Myzus persicae**	*Trialeurodes vaporariorum*
Glutathione S-transferase						
Glutathione S-transferase omega	1	2	1	ND	1 (0)	13
Glutathione S-transferase epsilon	0	0	0	ND	0	1
Glutathione S-transferase sigma	3	5	6(7)	ND	7 (8)	8
Glutathione S-transferase delta	2	11	1	ND	3 (2)	0
Glutathione S-transferase theta	1	2	2(4)	ND	2 (0)	0
Glutathione S-transferase Zeta	0	2(0)	1	ND	0	2
Glutathione S-transferase unknown	0	1 (3)	0	ND	0	0
Glutathione S-transferase microsomal	3	2	1	ND	2	2
Total	**10**	**25**	**12**	**ND**	**15**	**26**
Uridine diphosphate-GlycosylTransferase (UGT)						
UGTs	**35**	**55**	**16**	**76**	**38**	**42**
Carboxyl/Cholinesterase (CCE)						
Detoxification/dietary class	2	5	22	6	5	14
Pheromone/hormone processing	10	18	9	20	12	7
Neuro/developmental (total)	8	8	12	16	5	10
clade H - Glutactin	1	1	2	1	0	0
clade J - Acetylcholinesterase	2	2	2	4	3	3
clade K - Gliotactin	1	1	1	1	1	1
clade L - neuroligins	3	3	4	10	1	3
clade M - neurotactine	0	0	1	1	0	1
Unknown function	1	1	2	1	1	2
Total CCEs	**20**	**31**	**43**	**42**	**23**	**31**
ABC sub-family						
A	4	11	ND	8	ND	3
B	6	9	ND	3	ND	9
C	5	16	ND	6	ND	7
D	3	2	ND	2	ND	4
E	1	1	ND	1	ND	1
F	3	4	ND	3	ND	3
G	22	19	ND	23	ND	9
H	23	9	ND	9	ND	9
Total	**67**	**71****	**ND**	**55**	**ND**	**45**
Cytochrome P450 (CYP)						
clan2	7	10	5	10	10	7
clanmito	6	8	6	7	7	7
clan3	20	23	50	57	25	41
clan4	33	23	23	56	23	45
Total	**66**	**64**	**84**	**130**	**65**	**80**
Total detoxification genes number	**198**	**175**	**155*****	**333*****	**136*****	**224**

data for Bemisia tabaci : Chen et al 2016

A. pisum UGT sequences were reanalysed based on latest genome releases (AphidBase). Numbers in brackets denote number p

CYP data from A pisum are from Feyereisen R, 2011b

CYP data from M.persicae are from Dermauw et al. 2020

CCE data from B. tabaci from Xia et al, 2019 (number corrected compared to Chen et al, 2016: 51 CCE)

CCE data from R. prolixus from Schama et al, 2016 but assignment to clades were modified according to our phylogenetic analy

Trialeurodes vaporariorum Pym A. et al 2019 BMC Genomics

*Ramsey et al, 2010, number based on EST data

** Acyrthosiphon pisum, ABC transporter numbers obtained by automatic analysis.

***this data are incomplete

previously described UGTs in (Ramsey, Rider et al. 2010, Schama, Pedrini et al. 2016).

/sis (Schama et al, 2016: 22 class I and 9 class 2)

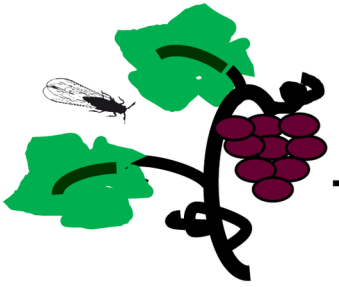

Manual annotation of Phylloxera genome

Gallicole and radicicole Phylloxera transcriptomic analysis

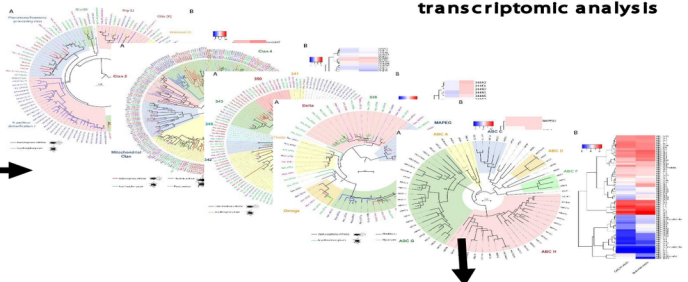

Key genes involved in phylloxera physiology and in adaptation to grapevine xenobiotics